A New Analytical Method for Measuring Hydrogen Isotopes Using GC-IRMS: Applications to Hydrous Minerals

by

Michael Robert Sheehan

A Thesis Presented in Partial Fulfillment
of the Requirements for the Degree
Master of Science

Approved April 2011 by the
Graduate Supervisory Committee:

L. Paul Knauth, Chair
Ariel Anbar
Jack Farmer

ARIZONA STATE UNIVERSITY

May 2011

ABSTRACT

A new analytical method is proposed for measuring the deuterium to hydrogen ratio (D/H) of non-stoichiometric water in hydrous minerals via pyrolysis facilitated gas-chromatography – isotope ratio mass spectrometry (GC-IRMS). Previously published analytical methods have reported a poorly understood nonlinear dependence of D/H on sample size, for which any accurate correction is difficult. This sample size effect been variously attributed to kinetic isotope fractionation within the mass spectrometer and peripheral instruments, ion source linearity issues, and an unstable H_3^+-factor or incorrect H_3^+-factor calculations.

The cause of the sample size effect is here identified by examinations of individual chromatograms as well as bulk data from chromatographic peaks. It is here determined that it is primarily an artifact of the calculations employed by the manufacturer's computer program, used to both monitor the functions of the mass spectrometer and to collect data. Ancillary causes of the sample size effect include a combination of persistent background interferences and chromatographic separation of the isotopologues of molecular hydrogen. Previously published methods are evaluated in light of these findings. A new method of H_3^+-factor and D/H calculation is proposed which makes portions of the Isodat software as well as other published calculation methods unnecessary.

Using this new method, D/H is measured in non-stoichiometric water in chert from the Cretaceous Edwards Group, Texas, as well as the Precambrian

Kromberg Formation, South Africa, to assess hydrological conditions as well as to estimate the maximum average surface temperature during precipitation of the chert. Data from Cretaceous chert are consistent with previously published data and interpretations, based upon conventional analyses of large samples. Data from Precambrian chert are consistent with maximum average surface temperatures approaching 65°C during the Archean, instead of the much lower temperatures derived from erroneous methods of sample preparation and analysis. D/H is likewise measured in non-stoichiometric water in silicified basalt from the Precambrian Hooggenoeg Complex, South Africa. Data are shown to be consistent with D/H of the Archean ocean similar to present day values.

DEDICATION

To my beautiful wife Cayley, for all of her love, support, and patience.

ACKNOWLEDGMENTS

First and foremost, I would like to thank Dr. L. Paul Knauth for sharing his boundless knowledge and for providing chert samples, for his patience during the many periods of technical difficulties, and for his assistance in the writing and editing process. I would also like to thank Karlis Muehlenbachs for contributing basalt samples and invaluable advice. In addition, I would like to thank Dr. Ariel Anbar and Dr. Jack Farmer for their assistance, flexibility, and good humor in reviewing my work. I would like to thank Stan Klonowski for giving me insight into the minutiae of mass spectrometers and their accompanying peripheral instruments, as well as for providing me the tools to question the validity of previously published data. Finally, I would like to thank my parents, Timothy and Maryann Sheehan, for encouraging me to return to Arizona State University to complete this thesis.

TABLE OF CONTENTS

Page

LIST OF TABLES

LIST OF FIGURES

Figure Page

Figure Page

Figure Page

Figure Page

Figure Page

1. Notation

In δ-value notation, the isotope ratio is given as a per mil deviation from the isotope ratio in a known standard reference material, as suggested by Urey (1948). In this notation scheme, $\delta = \left(\frac{R_{Sample}}{R_{Standard}} - 1\right) \times 1000‰$, where R is the ratio of the heavy isotope to the light isotope in the element of interest and all values of δ are expressed in per mil relative to a standard scale (McKinney et al., 1950). Using this practice, the δ-value of a substance enriched in the heavy isotope relative to the standard will be positive, whereas the δ-value of a substance depleted in the heavy isotope relative to the standard will be negative. For hydrogen and oxygen isotope ratios of water contained in solid samples, all values herein are reported relative to Vienna Standard Mean Ocean Water (VSMOW), as originally defined by Craig (1961a) and more narrowly defined by Coplen (1995). In addition, D/H or δD will denote the deuterium to hydrogen ratio, where D rather than ^{2}H indicates deuterium, as this has been the traditional representation in the literature. $^{18}O/^{16}O$ will be referred to directly or denoted $\delta^{18}O$. The fractionation factor, a measure of the amount of isotopic fractionation that will occur in an equilibrium isotope exchange reaction involving substances a and b, is given by $\alpha = \frac{R_a}{R_b}$. For the purposes of this thesis, α is considered to be dependent only upon temperature.

2. Analytical Method

2.1. Introduction

When measuring the deuterium to hydrogen ratio (D/H) of water extracted from geologic materials, the larger the sample the more prone it becomes to contamination by hydrogen-bearing weathering products and veins of fluid-containing secondary silicates. In the traditional method of measuring D/H in water extracted from geologic materials, sample sizes are often in excess of 1 gram. With the advent of pyrolysis facilitated gas-chromatography isotope-ratio-mass-spectrometry (GC-IRMS), it has become possible to measure D/H in water extracted from samples weighing less than 1 milligram. However, when attempting to utilize this method for liberating non-stoichiometric water by flash-heating of hydrous minerals, a strong nonlinear dependence of D/H on sample size is encountered. Large variations exceeding tens of per mil are observed at the smallest sample sizes (e.g. Hren et al., 2009). A method is therefore required to assess the actual D/H of water in such minerals. However, the conventional procedure is difficult to replicate because the amount of sample required for precise measurement cannot be predicted to any degree of certainty in minerals with variable, non-stoichiometric water content. In liquid samples, aliquots of a near constant volume are introduced into the instrument such that sample sizes are, for all intents and purposes, identical and easily referenced to a standard.

Thus, this sample size effect has not been recognized while analyzing D/H in liquid hydrocarbons or liquid water.

Descriptions of the sample size effect while using pyrolysis facilitated GC-IRMS systems have been reported by Sharp et al. (2001), Abruzzese et al. (2005) and Greule et al. (2008). These authors applied various empirical corrections to their data in an attempt to negate the effects of sample size on D/H. However, the various methods generate conflicting results depending upon both the initial conditions of the empirical correction and the range of sample sizes. Necessarily, in order to obtain reproducible results, the cause of this sample size effect must be identified and any correction to the data must be applicable across the spectrum of possible sample sizes. Of vital importance to any correction scheme is knowledge of the H_3^+-factor – the rate of production of the ion H_3^+ in the ion source of the mass spectrometer – and how it affects direct measurements of D/H in mass spectrometry. Here, I document the origin of the sample size effect, evaluate the empirical corrections used by Sharp et al. (2001) and Abruzzese et al. (2005), assess the validity of various methods of H_3^+-factor calculation, and specify a comprehensive experimental method and data reduction process that ensures future measurements of D/H made using pyrolysis facilitated GC-IRMS are both accurate and precise.

2.2. Background and Historical Development.

When analyte is produced in an apparatus that is directly connected to a mass spectrometer and fed immediately into the mass spectrometer without an intermediate storage and transfer step, both the system and the production of analyte is said to be online. In any other mass spectrometry system in which the analyte must be produced in a separate apparatus, stored, and then transferred to the mass spectrometer, both the system and the production of analyte is offline. In the earliest mass spectrometers used in the field of stable isotope geochemistry, the analyte was produced offline and introduced to the mass spectrometer as a gas at a constant pressure via a bellows connected to a single- or dual-inlet valve system. Quite the opposite of the traditional bellows systems, modern mass spectrometers are commonly continuous-flow systems, in which a laminar stream of inert gas entrains the analyte and conveys it to the ion source of the mass spectrometer at a constant pressure.

Friedman (1953) utilized an offline, dual-inlet gas-source mass spectrometer (DI-IRMS), to perform the first survey of D/H variations in natural waters. He produced hydrogen gas for analysis by reducing water over hot zinc granules in a vacuum line (Figure 1) according to the following reaction: $Zn + H_2O \leftrightarrow H_2 + ZnO$. All contaminants were condensed or frozen in a cold trap cooled with liquid nitrogen. The hydrogen gas was then pumped by a Toepler pump into a calibrated manometer. If the yield was quantitative, the gas was

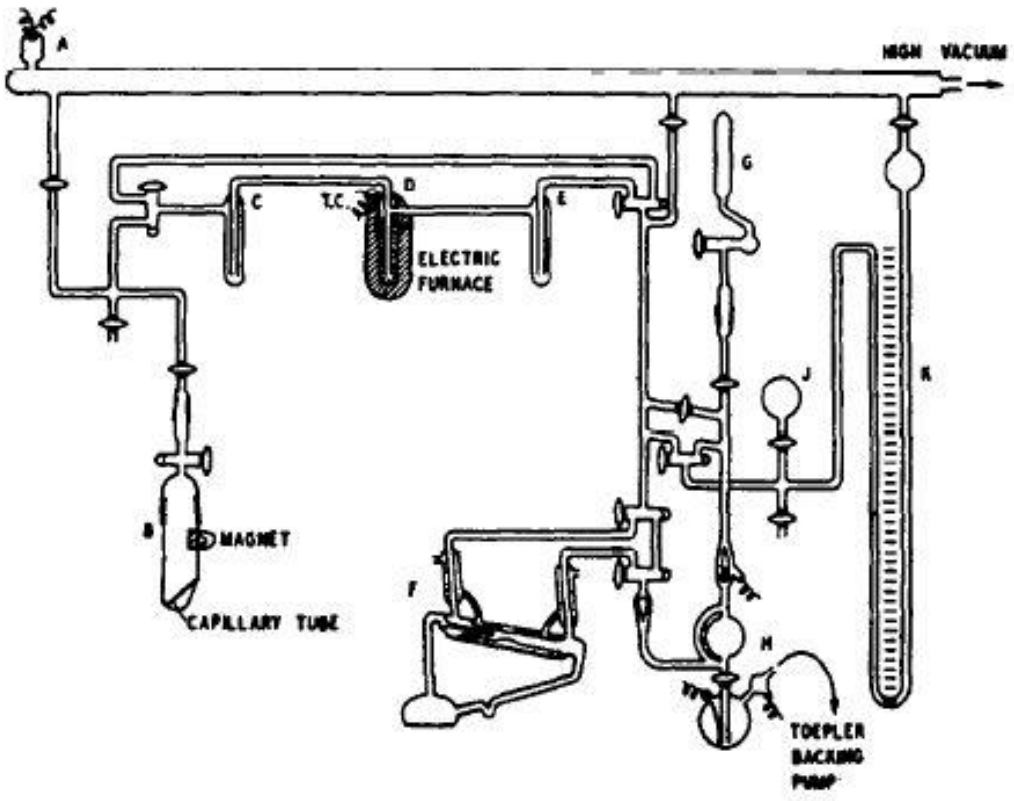

Figure 1. A vacuum line schematic from Friedman (1953). This vacuum line apparatus was used to generate hydrogen gas from water.

pushed into a sample tube for introduction into the ion source of the mass spectrometer.

Friedman (1953) compared the ratio of the signal strength of mass-3 (HD^+) to mass-2 (H_2^+) ions. Mass-4 (DD^+) was not considered relevant in determining the deuterium content of the gas because of the high statistical improbability that this ion would occur. The ratio of the signal strengths of mass-3 (HD^+) to mass-2 (H_2^+) was the observed value of R. The signal intensity, expressed in Volts, is the raw data produced by the mass spectrometer and represents the voltage generated by a continuous stream of ions of a given mass-to-charge ratio striking a Faraday Cup or other collector. For the remainder of this thesis, the signal intensity, the measured voltage generated by an ion of a given mass-to-charge ratio, will be expressed as V_x, where x is the value of the mass-to-charge ratio. In short then, Friedman (1953) initially measured R as $\frac{V_3}{V_2}$.

Based upon insights made by Nier (1947), Friedman (1953) noted that H_3^+ is produced in proportion to the pressure of hydrogen gas in the ion source of the mass spectrometer, according to the reaction described by Smyth (1931): $H_2^+ + H_2^0 \rightarrow H_3^+ + H^0$. As the pressure of molecular hydrogen in the ion source of the mass spectrometer increases, the number of H_2^+ ions increases and is measured as V_2. In turn, as the number of H_2^+ ions increases, the number of H_3^+ ions, measured as some unknown fraction of V_3, increases. The mass-to-charge ratio of the ions H_3^+ and HD^+ are nearly identical. The mass spectrometer used by Friedman (1953) was incapable of resolving H_3^+ from HD^+. Modern mass spectrometers

used in the field of stable isotope geochemistry are likewise incapable of resolving H_3^+ from HD^+. As a result, when the mass spectrometer's ion source facilitates the production of the ion H_3^+, the H_3^+ ion acts as an isobaric interference to the ion HD^+. V_3, then, is the sum of the voltage produced by both HD^+ and H_3^+. This has the effect of creating an anomalously high value of R which increases radically as V_2 increases.

Friedman (1953) determined that mechanical improvements to the mass spectrometer as well as more rigorous operational measures were necessary to minimize and account for the contribution of H_3^+ to V_3. First, rather than vary the total gas pressure within the ion source, he kept the gas pressure both low and constant. The partial pressure of hydrogen gas was varied, rather than the total pressure as in Nier (1947). The high vacuum within the mass spectrometer ensured that the partial pressure of molecular hydrogen was very low, inhibiting the production of H_3^+. Second, he added a repeller electrode to the ion source. This repeller plate provided an accelerating voltage to more rapidly eject the H_2^+ and HD^+ ions out of the ion source and into the mass analyzer, thereby reducing the probability of the Smyth reaction occurring for a given H_2^+ ion. Third, he increased the accelerating voltage to 2200 Volts; a very high operating voltage at the time. The high operating voltage likewise ensured a minimal residence time of ions within the ion source of the mass spectrometer. These mechanical enhancements markedly reduced the total number of H_3^+ ions produced in the ion source, ensuring that further corrections were more manageable. Finally, he

recognized that as he increased V_2 for a given sample, the value of R increased linearly where it should have been constant, assuming no contributions to V_3 from other sources. This indicated the possibility that the contribution of H_3^+ to V_3 could be accurately predicted for a given value of V_2.

Friedman (1953), using a laboratory standard hydrogen gas adjusted to various partial pressures and therefore different voltages, plotted R as a function of V_2, obtaining a curve of the form $R^* = kV_2 + R$ (Figure 2). In this curve, R^* was the observed value of $\frac{V_3}{V_2}$, k was the rate of H_3^+ production known contemporaneously as the H_3^+-factor, V_2 was the $\frac{m}{z} = 2$ signal voltage, and R was the value of $\frac{V_3}{V_2}$ for which the ion H_3^+ did not contribute to V_3. R, the value of $\frac{V_3}{V_2}$ at $V_2 = 0$, could not possibly have contained any contribution from H_3^+ because no H_2^+ ions were present. From this, Friedman (1953) reasoned that R, the intercept of his curve, was the voltage ratio containing contributions from only H_2^+ and HD^+, and was therefore the true isotope ratio of the hydrogen gas. In practice, Friedman plotted R^* as a function of V_2 using a laboratory standard gas. For measurements of unknown samples, he solved the equation for R (above) using the H_3^+-factor calculated during the measurement of his laboratory standard. The determination of the H_3^+-factor in the measurement of D/H is paramount, and depends solely upon the configuration of the ion source parameters. Friedman (1953) thus reported the first reproducible measurements of D/H variations in molecular hydrogen derived from water. He not only reported the deuterium

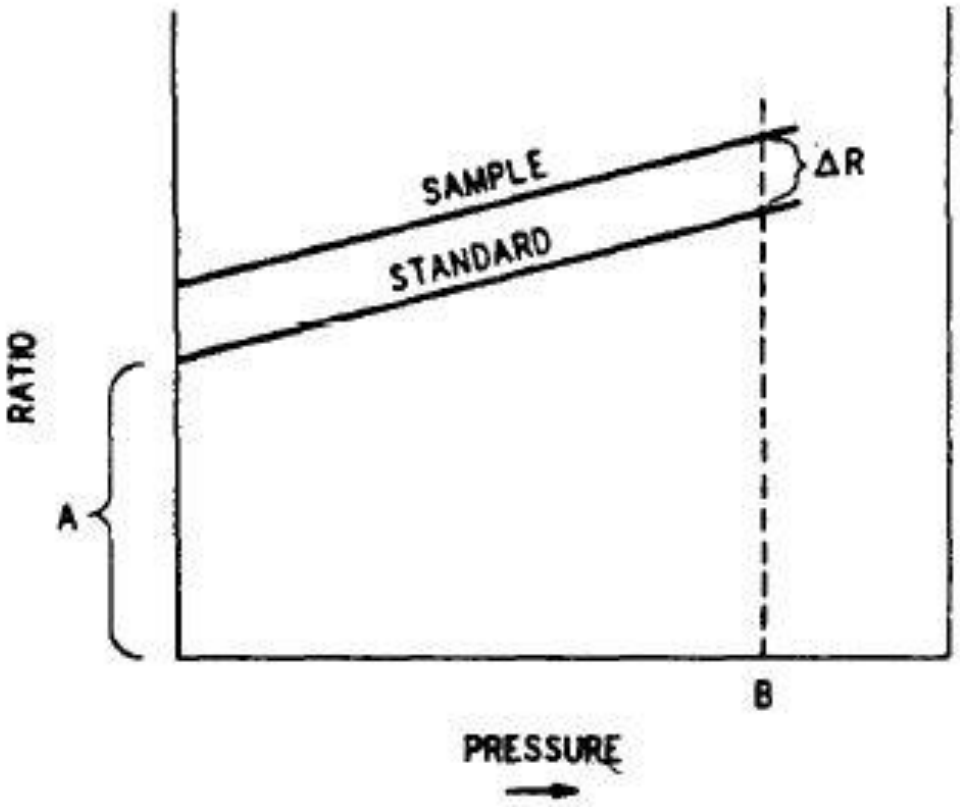

Figure 2. Isotope ratio as a function of pressure (from Friedman, 1953). Pressure, in this case, is a proxy for V_2. The increasing ratio indicates contribution to V_3 from H_3^+.

content of a number samples of marine and meteoric waters, he described a correction to the raw instrument-derived data necessary for accurate and precise measurements of D/H that could be applied to any DI-IRMS system.

The commonly accepted method of extracting water from hydrous minerals and reducing it to hydrogen gas for mass spectrometric analysis was described by Godfrey (1962). Godfrey (1962) simply extended the method originally described by Bigeleisen et al. (1952) and modified later in Friedman (1953). In this extraction method, water is obtained from a mineral or rock by heating under high vacuum using a high frequency induction heater coil (Figure 3). The water is then reduced over uranium granules that have been heated to 750°C, analogous to the zinc method used by Friedman (1953). According to Bigeleisen et al. (1952), uranium was used because of its known hydration states and smaller likelihood of memory effects. All undesirable condensates and gases were collected in a cold trap cooled with liquid nitrogen. The hydrogen gas was then measured and captured in a receiving bulb, using a Toepler pump, and transferred to the mass spectrometer. Godfrey (1962) used this method to measure δD in the magmatic minerals biotite, chlorite and hornblende from various geological provinces in order to further explore the concept of juvenile water. Although the method was effective, a single analysis was both time consuming and labor intensive.

The primary source of error in the method of δD measurement described by Godfrey (1962) was the inclusion of undesirable material in the sample

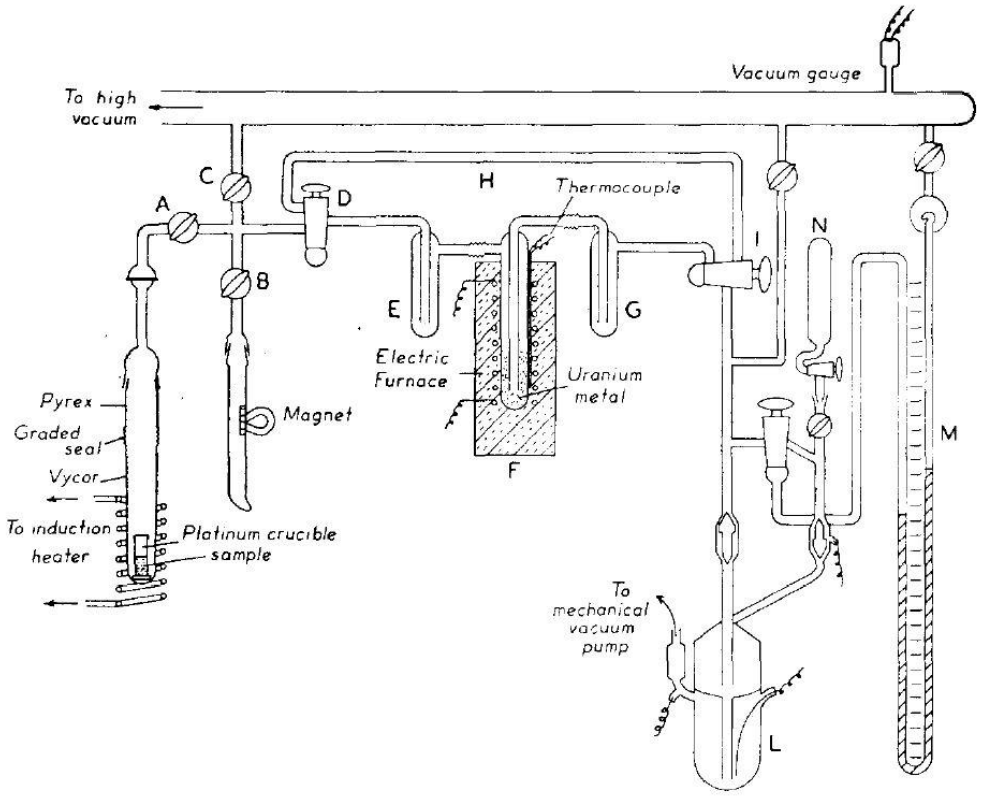

Figure 3. Vacuum line used for extracting water from geologic samples (from Godfrey, 1962)

undergoing analysis. For example, secondary mineral veins or weathering crusts containing water or other hydrogen-bearing compounds could be inadvertently included in the sample. The inclusion of contaminant material often occurred as a result of the large amount of material required in order to generate amounts of water adequate to produce a sufficient volume of hydrogen gas; oftentimes several grams of solid material or more. In addition to the error generated by contamination, a new water sample could equilibrate isotopically with water that had failed to react in the previous analysis. This is a source of a memory effect and resulted in some analyses possessing a value of δD that was a mixture of previous samples and the current. Nevertheless, used with care, the method proposed by Godfrey (1962) became the standard for extracting water from geological samples. Combined with Friedman's (1953) mass spectrometric method of δD determination, Godfrey (1962) prompted immediate exploration of the natural abundance of deuterium in water extracted from geological materials. All the same, the method was labor intensive, time consuming, and prone to occasional error. A more rapid, automated technique using smaller samples was desirable.

Matthews and Hayes (1978) were the first to describe the online production of gas for analysis by GC-IRMS. In their study, they connected a gas chromatograph (GC) to a 750˚C cupric-oxide combustion furnace, which in turn fed into a computer-controlled Varian CH-7 mass spectrometer (Figure 4). A sample gas containing carbon and nitrogen was purified and separated

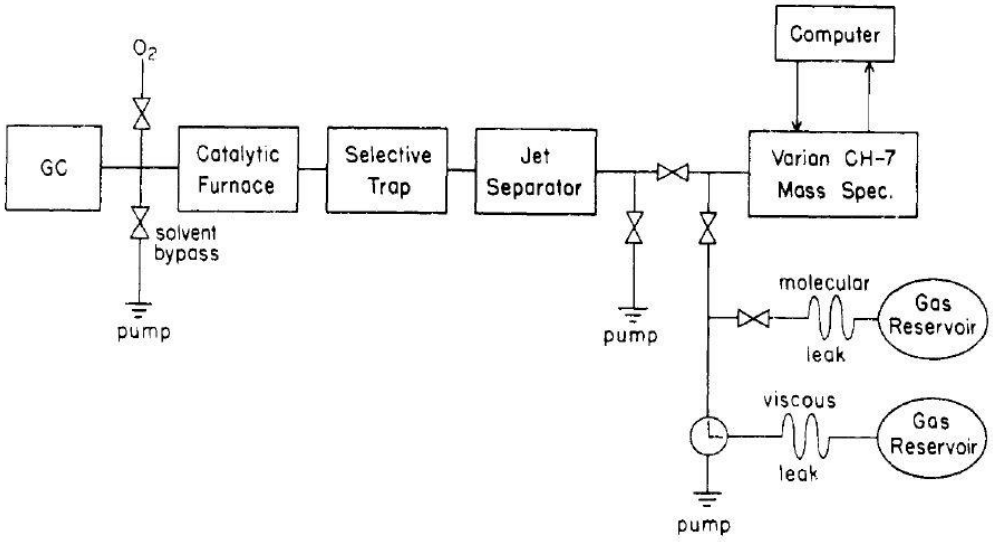

Figure 4. Block diagram indicating the placement of peripheral instruments relative to the mass spectrometer in the earliest GC-IRMS system (from Matthews and Hayes, 1978).

chromatographically, passed through a combustion oven to produce CO_2 or N_2, then the isotope ratios of carbon and nitrogen were measured by the mass spectrometer. The transfer of analyte from the gas chromatograph to furnace required that it be entrained in a laminar stream of inert gas. Helium was chosen because of its availability and low mass-to-charge ratio, guaranteeing little to no interference with measurement of the desired isotopes. The stream of helium is kept at a constant pressure such that the analysis of a single sample is rapid and the chromatographic peak shape is relatively invariant. Were it bled directly into the mass spectrometer by diffusion, each analysis would take an inordinate amount of time and the peak shape would be unstable and irreproducible.

When a sample gas passes through a chromatograph, the retention and exit time of the constituent compounds may be significantly different. Matthews and Hayes (1978) exploited this interval by rapidly changing the ion source and mass analyzer settings of the mass spectrometer using a computer, such that $\delta^{13}C$ and $\delta^{15}N$ could both be measured during the course of a single analysis. As a direct result of the online production and short duration of a chromatographic peak, much smaller sample sizes are typically required in GC-IRMS. This reduces the probability of the aforementioned error that can result from very large samples.

The method of chromatographic peak evaluation – the determination of the start and end of a chromatographic peak in GC-IRMS systems – was described by Ricci et al. (1994). Working in conjunction with Finnigan MAT (currently Thermo Finnigan), the authors described elements and general

characteristics of the computer program, "Isodat," which is used by most commercial GC-IRMS systems to evaluate chromatographic peaks and calculate δ-values. Integrated data points representing V_x, plotted as a function of time, comprise a chromatographic peak. In their study, the authors state that the start of a chromatographic peak is determined by a calculation of the instantaneous rate of change at a point along the dynamic time integrated curve generated by the signal associated with the more abundant (and usually lighter) isotope. The slope is determined by a 5-point regression. Figure 5 provides a schematic illustration of a chromatographic peak, as well as the 5-point regression used to calculate peak commencement. After a critical slope threshold is reached, the chromatographic peak begins. Because of the relatively high integration interval of the data points that comprise a chromatogram (0.2 s), Isodat estimates the value of the maximum peak amplitude of any chromatographic peak by fitting a series of parabolas to the apex of the chromatographic peak. Based upon data collected in this study, this method appears to be very accurate. After the maximum amplitude of the chromatographic peak has been reached, a negative critical slope threshold determines its termination. This slope threshold can be modified by the user, but is typically preset and not altered. The static background levels of the instrument are determined by averaging the 4 data points prior to the start of the chromatographic peak (Figure 5).

Concurrent with the measurement of intensity, Isodat records the instantaneous signal ratio. Figure 6 illustrates a series of four chromatographic

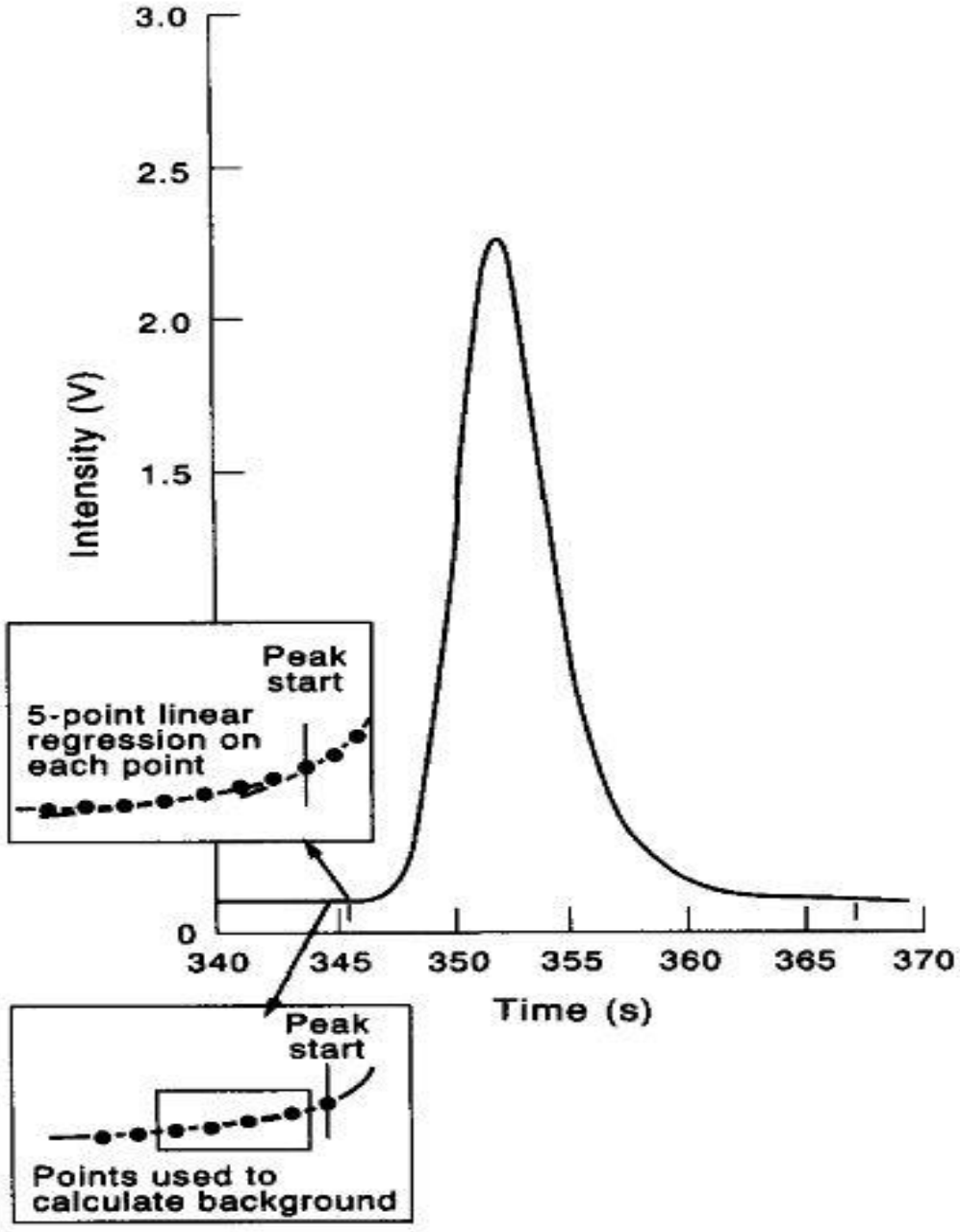

Figure 5. A schematic of a hypothetical chromatographic peak, showing both the method of peak-start and background level determination (from Ricci et al., 1994).

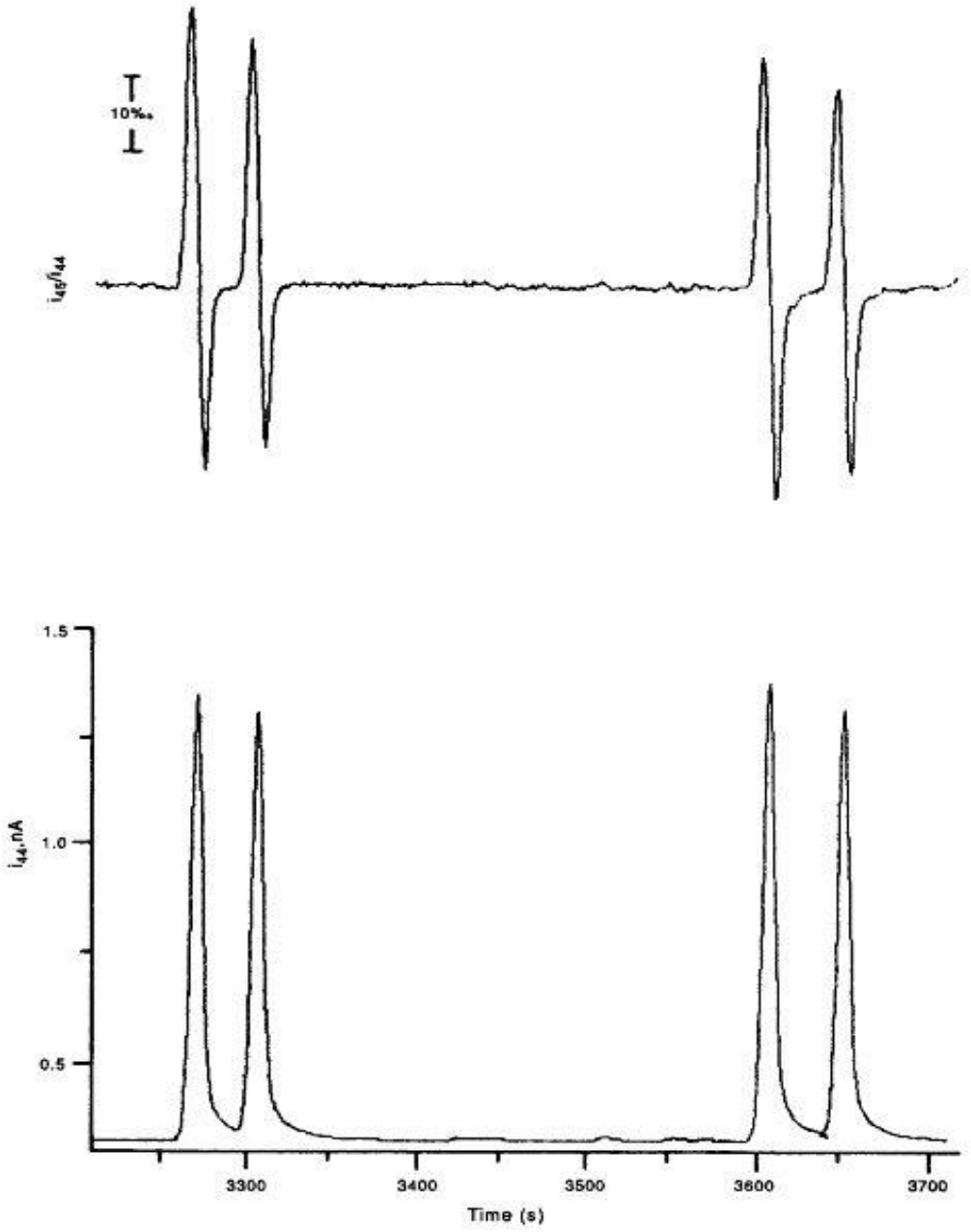

Figure 6. A set of chromatographic peaks with the instantaneous isotope (46/44) ratio plotted as a function of time (from Ricci et al., 1994).

peaks accompanied by the instantaneous isotope ratio of carbon dioxide gas. The δ-value of a sample is determined by calculating the arithmetic mean of the data points that comprise the instantaneous signal ratio over the duration of the chromatographic peak. The large range in value of the instantaneous ratio is due to chromatographic separation of the isotopologues of carbon dioxide. The mean value is then multiplied by a factor and offset relative to an arbitrary δ-value assigned to a monitoring gas. The multiplicative factor and the offset are used to fit outputted data to the arbitrarily assigned scale of the instrument (Sharp, 2007). The monitoring gas is analyzed along with samples and standards in order to track the performance of the instrument. The δ-value of the monitoring gas may be assigned such that the outputted δ-value of an unknown sample falls on an acceptable scale, such as VSMOW or VPDB.

From 1978 until 1995, the primary elements for isotope ratio measurement by GC-IRMS were carbon and nitrogen. Hydrogen, however, is a very desirable element for isotopic analysis because of its utility as a hydrological tracer and because of its importance in climatological studies. However, considerable difficulties in the online production of hydrogen and its isotope ratio measurement in continuous flow systems made the validity δD measurements using GC-IRMS questionable at best. In the mass spectrometers used for GC-IRMS between 1978 and 1995, it was difficult, if not outright impossible, to resolve H_2^+ from HD^+. Prosser and Scrimgeour (1995) remedied this by modifying a Europa Scientific 20 – 20 isotope ratio mass spectrometer. They simply added an additional collector

spur with a large enough dispersion to resolve these ions. However, this was only a partial solution to the overall problem. When helium was used as a carrier gas in hydrogen isotope measurement, $^4He^+$ tended to overlap somewhat with HD^+, creating large, unpredictable values of V_3.

Tobias et al. (1995) used two methods to eliminate the issue of helium overlap on the HD^+ signal: the use of an Argon carrier gas, rather than helium, and the use of a palladium foil filter designed to deflect helium and other ions while absorbing hydrogen gas and creating a hydrogen gradient, allowing it to pass in to the collectors. These modifications made possible, for the first time, the measurement of hydrogen isotope ratios by GC-IRMS. Modern mass spectrometers now use both an additional collector spur with a high dispersion as well as some sort of electrostatic filter (Sharp, 2001).

Prosser and Scrimgeour (1995) proposed the offline equilibration of hydrogen gas with water using a platinum-on-alumina catalyst. This method of analyte production took approximately three days to complete for a water of unknown isotopic composition, and thus did not achieve the goal of rapid, online analysis. In fact, it could be argued that this method of analysis was far more time consuming and much more poorly understood than the analysis of hydrogen derived from water by conventional DI-IRMS as described by Friedman (1953) and Godfrey (1962). Tobias et al. (1995), on the other hand, designed a two-furnace system in which one combustion furnace was loaded with Pt and CuO metal designed to produce CO_2 and H_2O from organics, and the second was

loaded with Ni to reduce water to hydrogen gas. The effluent was then passed through a Varian 3400 Gas Chromatograph, into an open-split (a tube open at one end and pressurized by the carrier gas into which a capillary from the mass spectrometer samples gas from capillaries that exit the gas chromatograph), and into the ion source. However, it was determined that at this temperature, reduction of water to produce hydrogen gas was not quantitative. Nevertheless, Tobias et al. (1995) did report reproducible data and thus designed one of the first rapid, online hydrogen-producing apparatuses used in GC-IRMS.

Werner et al. (1996), were the first to use the now commonplace furnaces containing glassy carbon to produce carbon monoxide and molecular hydrogen via the reaction $C + H_2O \rightarrow CO + H_2$. This type of pyrolysis reaction is the hallmark of modern D/H measurement in GC-IRMS. Nevertheless, Werner et al. (1996) did not measured δD. Rather, they measured $\delta^{18}O$ by determining the isotope ratio of oxygen in CO^+. Begley and Scrimgeour (1997) were the first to use a pyrolysis reaction to produce hydrogen in order to determine δD in water. In their system, a microfurnace containing nickel coated with carbon was used to reduce water to hydrogen gas in a pressurized helium atmosphere.

In GC-IRMS, R has been measured both by comparing the amplitude of the chromatographic peaks at given points in time or by comparing the total area (A_x) under the chromatographic peaks. Begley and Scrimgeour (1997) calculated the H_3^+-factor of their instrument by plotting $\frac{A_3}{A_2}$ as a function of the maximum value of V_2 (the chromatographic peak amplitude) during individual injections of

0.3, 0.5, and 0.7 µl of local tap water, and then followed the calculations outlined in Tobias and Brenna (1996a, 1996b). This was a relatively small range in sample size, and produced useable data for fixed-volume injections of water.

It should be noted that prior to 2001 all publications of pyrolysis GC-IRMS analyzed fixed volumes of liquids or gases. Sharp et al. (2001) were the first to publish a method of δD measurement in non-stoichiometric water extracted from geological samples using pyrolysis. The combination dual-inlet/continuous-flow instrumentation described by Sharp et al. (2001) was essentially a modified version of the commercially available instrumentation currently in common use (Figure 7). Sharp et al. (2001) were the first researchers to use a Thermo Finnigan high Temperature Conversion Elemental Analyzer (TC/EA) coupled with a mass spectrometer to measure δD in water derived from geologic materials. The TC/EA is a vertical tube furnace with a tungsten-carbide heating element operated at approximately 1450°C. A ceramic tube is inserted into the furnace and houses a glassy carbon tube. A Costech Zero Blank Autosampler is connected to the top of the ceramic tube and delivers samples to the TC/EA. The ceramic tube is sealed from the atmosphere and pressurized with helium. Hydrogen is liberated from the sample via pyrolysis. Helium acts as a carrier gas as in other GC-IRMS systems. The entrained hydrogen gas is then passed through a 5Å molecular sieve where it is purified and separated. From the gas chromatograph, the hydrogen gas is passed through an open-split and into the ion source of the mass spectrometer. Sharp et al. (2001) measured δD and $\delta^{18}O$ in

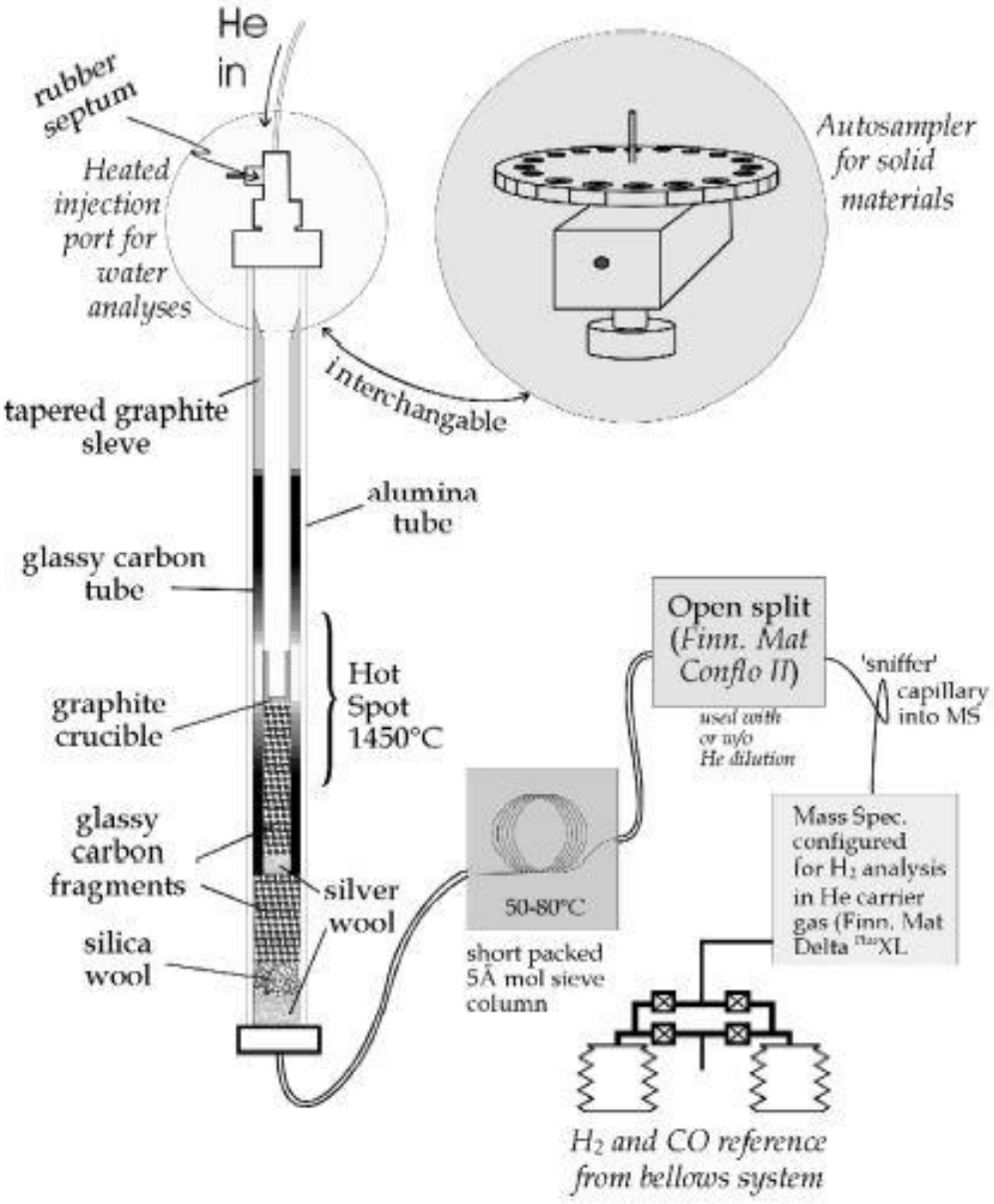

Figure 7. Schematic of a Thermo Finnigan TC/EA connected via a Finnegan Conflo II to a mass spectrometer (from Sharp et al., 2001).

water from a kaolinite laboratory standard and the National Institute of Standards and Technology (NIST) biotite standard, NBS-30. The system utilized by Sharp et al. (2001) was not entirely online, however, as standard gases used to both calibrate the instrument and act as references to unknown samples were introduced via a bellows.

Isodat is the software used to both control the functions and parameters of the mass spectrometer as well as to monitor, automatically correct, and report data to the user (Ricci et al., 1994). Isodat is used in most commercial GC-IRMS systems, and is used here as well as by previous workers (e.g. Sharp et al., 2001; Abruzzese et al., 2005; Hren et al., 2009). Isodat calculates the H_3^+-factor by evaluating δD in a series of chromatographic peaks of a single gas at varying partial pressures, iterating through a series of values. In this calculation method, a peak is defined as the reference peak by the experimenter. The value of the H_3^+-factor is selected that most effectively reduces the absolute error of the measured δ-value of the remaining chromatographic peaks, such that the measured δ-values of all chromatographic peaks closely approach the arbitrary value assigned by the experimenter. This process follows the method outlined by Sessions et al. (1999). The experimenter may also enter a H_3^+-factor value manually. Sharp et al. (2001) manually input a value for the H_3^+-factor using the H_3^+ correction tool in Isodat. They select the value through trial and error that best produces no correlation between the Isodat-outputted value of δD and V_2 (Figure 8).

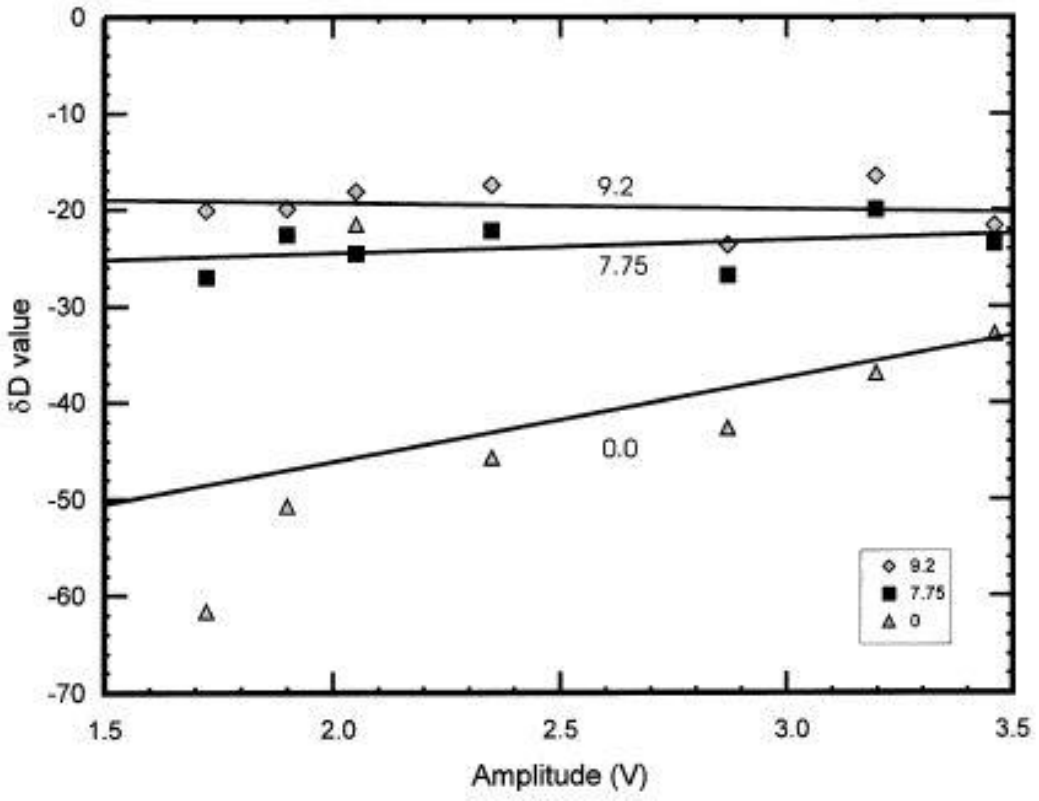

Figure 8. δD as a function of chromatographic peak amplitude. The values shown on the figure represent the H_3^+-factor inputted manually into Isodat (from Sharp et al., 2001).

Sessions et al. (2001a, 2001b) provided a new interpretation of the H_3^+-factor based upon Sessions et al. (1999) as that value which minimizes the absolute error in the δD value of chromatographic peaks of different size. Additionally, Sessions et al (2001a, 2001b) suggest possible methods to correct for the contribution of H_3^+ to V_3 in GC-IRMS. Sessions et al. (2001a) proposed four possible methods to determine the H_3^+-factor in GC-IRMS: the Bellows Method, Peak-rms Method, Peak-slope method, and the Instantaneous Method. The Bellows Method is the method outlined by Friedman (1953), reevaluated on modern mass spectrometers. The Peak-rms Method is the method of choice employed by Sessions et al. (1999), and is identical to the method used by Isodat. The Peak-slope Method is identical to the Peak-rms method, except that rather than minimizing the absolute error, the H_3^+-factor is varied until no correlation exists between δD and sample size (although over a relatively small range of sample sizes) as in Sharp et al. (2001). Finally, in the Instantaneous Method, analyte gas is injected slowly into the reduction furnace, and the resulting broad chromatographic peak is integrated over intervals lasting 62 milliseconds. R is plotted as a function of V_2 and the H_3^+-factor is determined for each point along the curve. V_3 is then corrected accordingly. Sessions et al. (2001a) reported that they were unable to test this last method satisfactorily because of instrumental limitations.

Abruzzese et al. (2005) used the commercial instrumentation similar to that used by Sharp et al. (2001), however, they did not make use of the

bellows/dual-inlet portion of the instrument. Raw data from the 2005 publication and helpful comments concerning their method of H_3^+-factor determination and correction as well as final data reduction methods were provided by C.P. Chamberlain (personal communication). According to Chamberlain, Abruzzese et al. (2005) determined and corrected their data for the contribution of H_3^+, by using the Isodat H_3^+-factor correction tool. Subsequent analyses proceed using this H_3^+-factor. A calibration curve to account for sample size effects was established by analyzing 5 samples of a laboratory standard at various sizes. $\delta D_{Laboratory}$, outputted by Isodat from the analyses of the working standard, is plotted as a function of chromatographic peak area, A_2, expressed in units of V·s. The resulting curve, the best fit of which is in the form $y = -\ln(x)$, is used to normalize all of the analyses for that day to an arbitrary value of A_2 that falls within the range of the data comprising calibration curve (Figure 9). Since 2005, publications using pyrolysis facilitated GC-IRMS to measure D/H in water from solid samples correct for the contribution of H_3^+ and calculate δD-values using the methods outlined by either Sharp et al. (2001) or Abruzzese et al (2005).

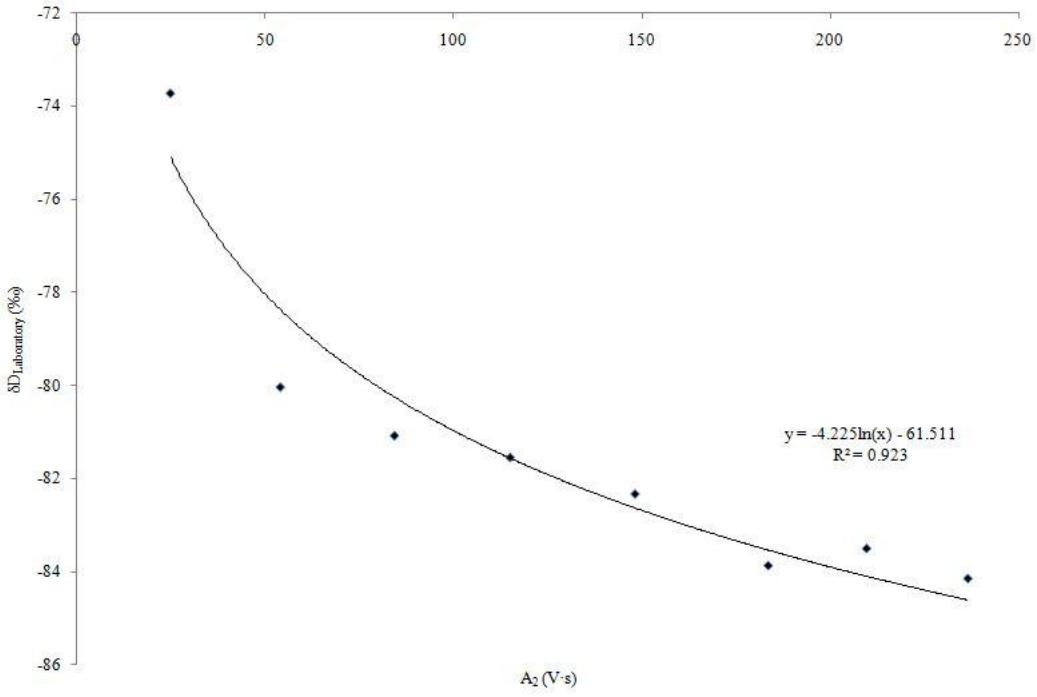

Figure 9. Nonlinear dependence of the observed isotope ratio on sample size. The data is from NIST standard NBS-30.

2.3. Current Problems and Resolutions

2.3.1. Isodat Functionality

The TC/EA peripheral instrument, coupled with a mass spectrometer, was originally designed for the measurement of hydrogen and oxygen isotope ratios in liquid water and liquid hydrocarbons; e.g. Tobias et al. (1995), Tobias and Brenna (1996a and 1996b), Begley and Scrimgeour (1997), and Burgoyne and Hayes (1998). Typically, a fixed volume of liquid is injected through a heated septum into the TC/EA. For the measurement of isotope ratios in waters, water standards are used. Likewise, for the measurement of isotope ratios in hydrocarbons, hydrocarbon standards are used. For the measurement of δD in waters and other liquids, a fixed injection volume is used for all unknowns and water standards. Thus, the sample size is approximately constant. As a result, in previous research in which liquids were analyzed, sample size was not noted to affect D/H in pyrolysis facilitated GC-IRMS. However, it has been reported that in the analysis of hydrous minerals containing non-stoichiometric water using pyrolysis facilitated GC-IRMS, D/H exhibits a strong nonlinear dependence upon sample size (e.g. Sharp et al., 2001; Abruzzese et al., 2005; Greule et al. 2008; C. Page Chamberlain, personal communication). It is shown here that the sample size effect is due to the calculation method used by Isodat to determine δD and the H_3^+-factor combined with small but persistent background levels of both V_2 and V_3

as well as chromatographic offset and peak shape variation of the isotopologues of hydrogen gas.

A chromatographic peak is comprised of hundreds to potentially thousands of data points, each representing an integration time of approximately 0.2 seconds or less. According to Ricci et al. (1994), Isodat calculates a δ-value by first calculating the arithmetic mean of the instantaneous isotope ratio over the entirety of a chromatographic peak. The mean value of the raw instantaneous isotope ratio is considered to be a proxy for the ratio of the total chromatographic peak area. In this thesis, the mean value of the instantaneous isotope ratio has never been observed to approximate the ratio of the chromatographic peak area. It is therefore unlikely that the H_3^+-factor calculation proposed by Begley and Scrimgeour (1997) accurately reflects the H_3^+-factor associated with their instrument. Nevertheless, after having taken the average instantaneous ratio, Isodat converts that number to a raw δ-value. The equation used is difficult to determine to a high degree of certainty, but a best fit curve applied to data from the international standard NBS-30 results in an approximate equation of $\delta D_{Raw} = 23 \times R_{Average} + 37$, with $R^2 = 0.912$ (Figure 10). Error is due to difficulties in exactly reproducing the correct duration of the peak; integration units in the chromatogram are assigned numeric labels that do not always precisely correspond to the integration time. This raw δ-value is then adjusted according to an arbitrary δ-value assigned to a monitoring gas. In the system used in this thesis, the monitoring hydrogen gas was arbitrarily assigned a value of –130‰,

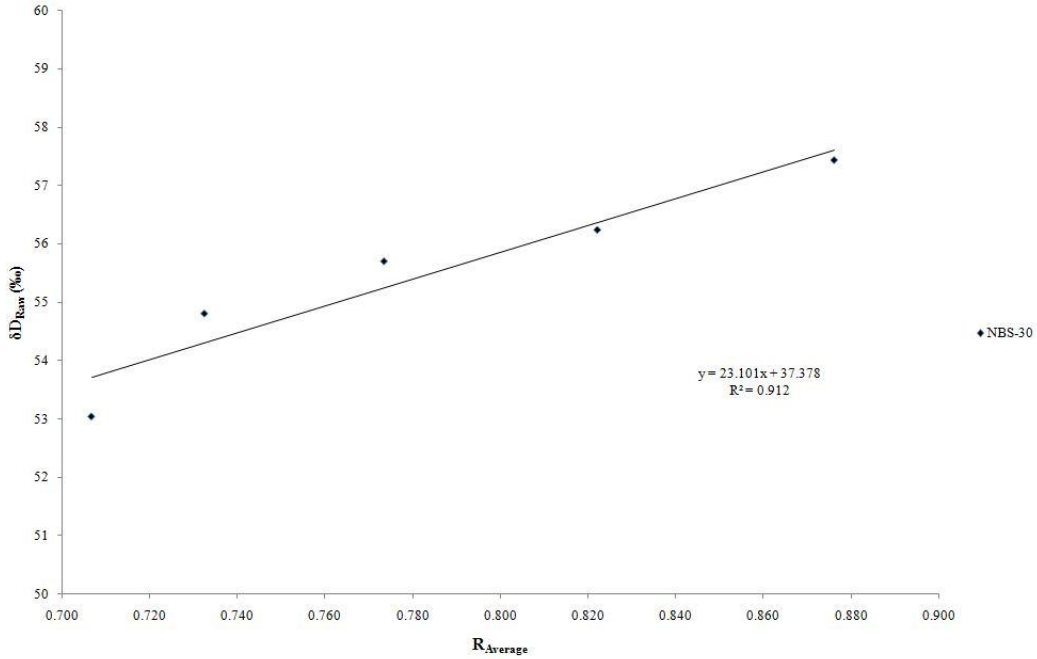

Figure 10. The observed value of δD as a function of the average instantaneous isotope ratio of a chromatographic peak.

which is utilized by Isodat via the following equation: $\delta D_{Laboratory} = \frac{7}{8}\delta D_{Raw} - 130$ (Figure 11). From this laboratory value, data may be extrapolated to the VSMOW scale following the equation outlined by Sharp et al. (2001) and Sharp (2007): $\delta D_{Accepted} = a\delta D_{Laboratory} + b$. In practice, NIST standards or laboratory standards of known δD are analyzed and the accepted value of δD on the VSMOW scale is plotted as a function of the laboratory value. The values of a and b are determined using a best fit line and will vary according to the arbitrary value of δD assigned to the monitoring gas. To determine the accepted δD value of an unknown sample on the VSMOW scale, $\delta D_{Laboratory}$ is substituted into the equation once the values of a and b have been determined.

2.3.2. Persistent Background Effect

In the commercial GC-IRMS instrumentation used in recent publications (Sharp et al. 2001; Eiler and Kitchen, 2001; Abruzzese et al., 2005; Greule et al., 2008; Hren et al., 2009) there is a constant positive background value of both V_2 and V_3 even in the most ideal conditions. The background value of V_2 is most likely a result of minor signal overlap of the helium carrier gas, minor amounts of hydrogen gas present in the helium carrier gas, as well as minor amounts of H_2^+ that continually vent from the glassy carbon tube in the TC/EA. Typically, the background level is less than 0.050 V for the apparatus used in this work. The background value of V_3 is most likely due to signal overlap of the hydrogen

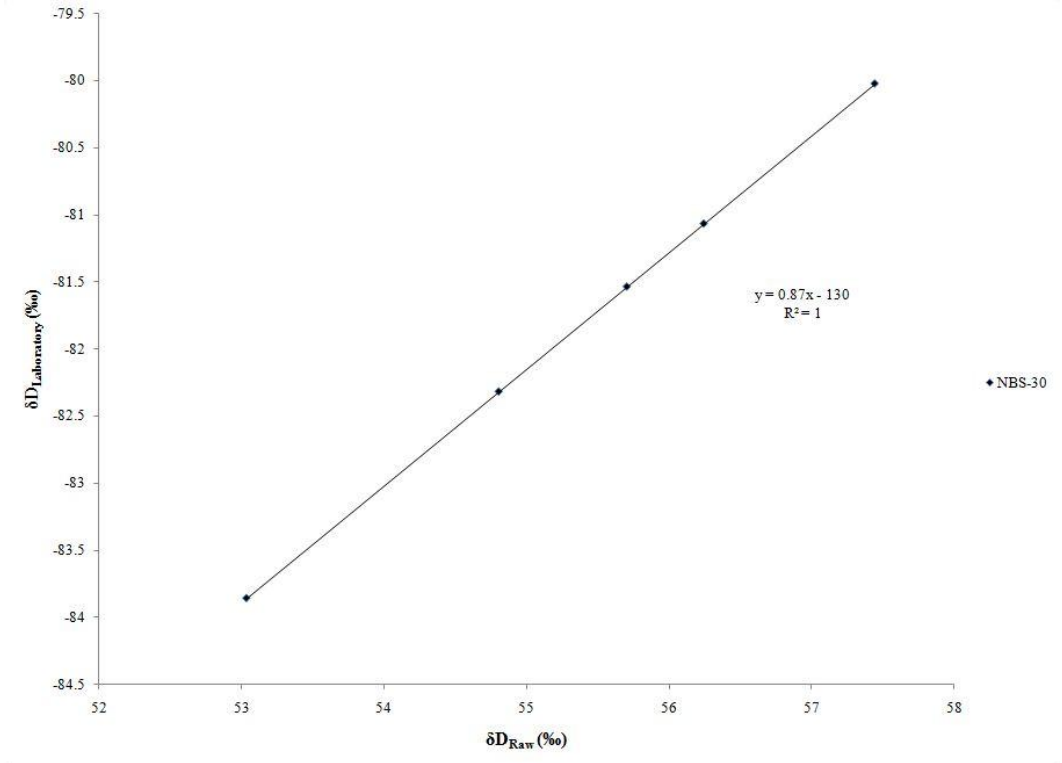

Figure 11. $\delta D_{Laboratory}$ as a function of δD_{Raw}. This illustrates the calculation used by Isodat to adjust a raw value to the arbitrary value of a monitoring gas.

carrier gas, minor amounts of hydrogen present in the helium carrier gas, as well as minor amounts of H_3^+ resulting from the H_2^+ that continually outgases from the glassy carbon tube. The V_3 signal is amplified by 10^3, and typically falls within 0.060 to 0.120 V. The signal amplification is neither corrected for nor altered in any way during Isodat's data compilation and calculations.

During the first few seconds of a chromatographic peak, the value of V_3 will commonly remain higher than the value of V_2. The raw instantaneous isotope ratio during these first several seconds of a chromatographic peak will be very high relative to the remainder of the peak – typically between 1.2 and 1.6. In relatively small chromatographic peaks, this period of high instantaneous isotope ratio will constitute a greater proportion of the entirety of the chromatographic peak than will be the case in very large chromatographic peaks. This can be expressed in terms of a mixing curve between the instantaneous isotope ratio of the persistent background and the analyte (Figures 12 and 13) In Figure 12 $R_{Average}$, the average of value of the instantaneous isotope ratio of a chromatographic peak, is expressed as a function of chromatographic peak area (A_2). In Figure 13, δD_{Raw}, the unadjusted δ-value calculated by Isodat, is likewise expressed as a function of A_2. In comparing both Figures 12 and 13 to Figure 9, it is clear that the constant background levels, combined with Isodat's method of δD calculation, are the primary source of the nonlinear dependence of δD upon sample size in pyrolysis facilitated GC-IRMS.

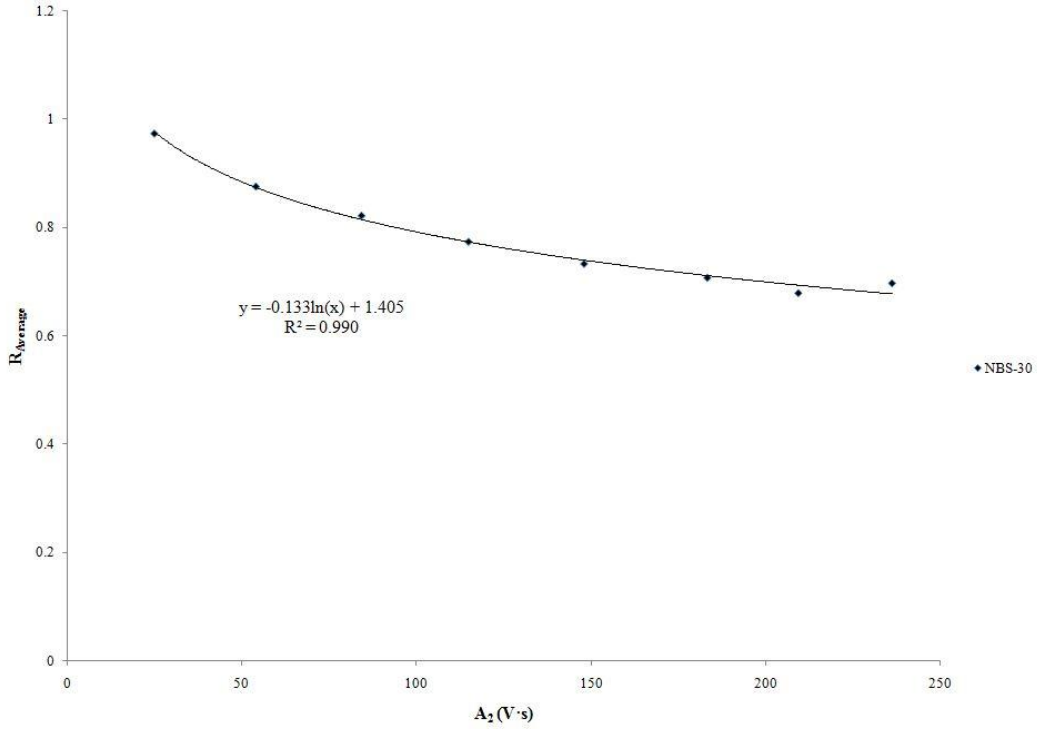

Figure 12. The average instantaneous isotope ratio of NBS-30, as determined from analysis of chromatogram data, at various sample sizes.

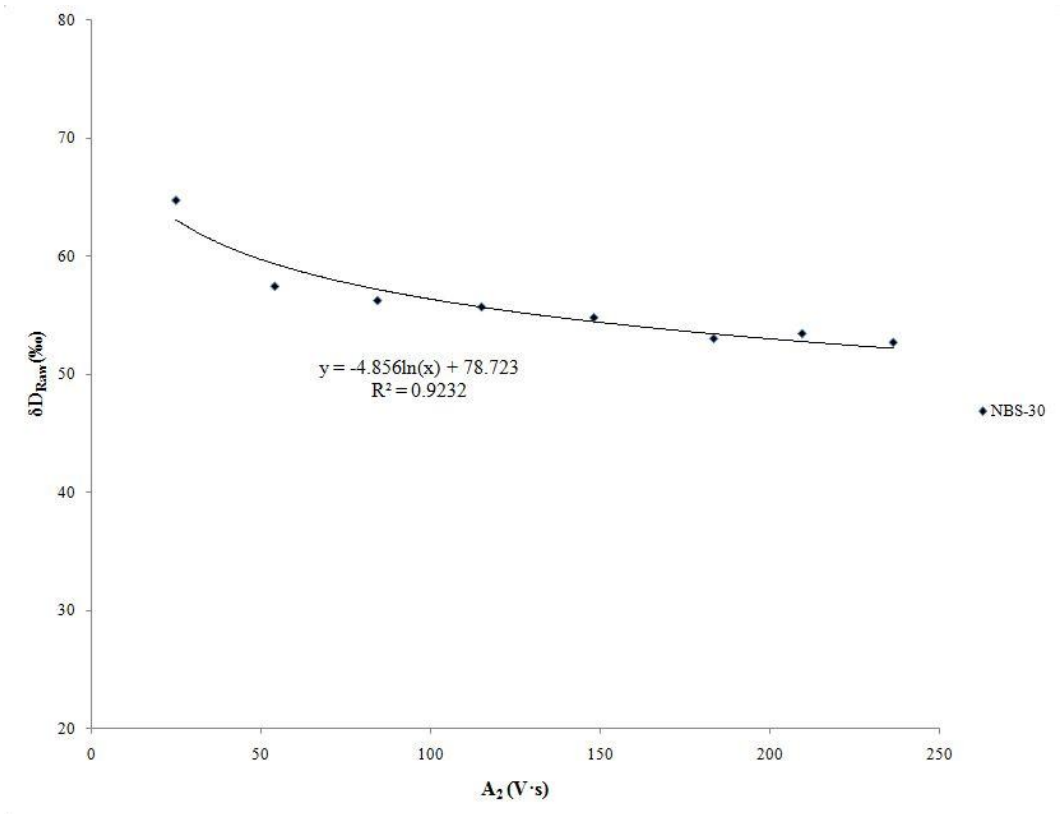

Figure 13. δD_{Raw} as a function of sample size for NBS-30.

2.3.3. Examination of Chromatogram Datasets

To confirm the above, a series of chromatogram datasets from a given material analyzed at various sample sizes may be used. A chromatogram dataset consists of a sequence of data points that comprise a chromatographic peak (Figure 14). The lobate appearance of the curves and the inflection point at the maximum peak amplitude of V_2 is due to chromatographic separation of the isotopologues of hydrogen gas, as described in Van Hook (1967), and summarized subsequently. In Figure 14, the contribution to V_3 from H_3^+ has not been corrected. It should be noted that R is greatest at the lowest signal intensity. For all of the chromatographic peaks represented in Figure 14, the number of data points between 0 and 1 V are approximately equal. As chromatographic peak size increases, the number of data points that extend past 1 V increases. The result, if R is plotted as a function of sample size, is an inverse mixing curve (Figures 9, 12, and 13). This is the primary cause of the sample size effect that has so plagued applications of this method to hydrous minerals.

2.3.4. Evaluation of Isodat Correction Tool

The sample size effect is exacerbated by under-correction of the contribution of H_3^+ to V_3 by the Isodat H_3^+-factor correction tool. As shown in Figure 14, following the initial precipitous drop in R, the value of R increases as a

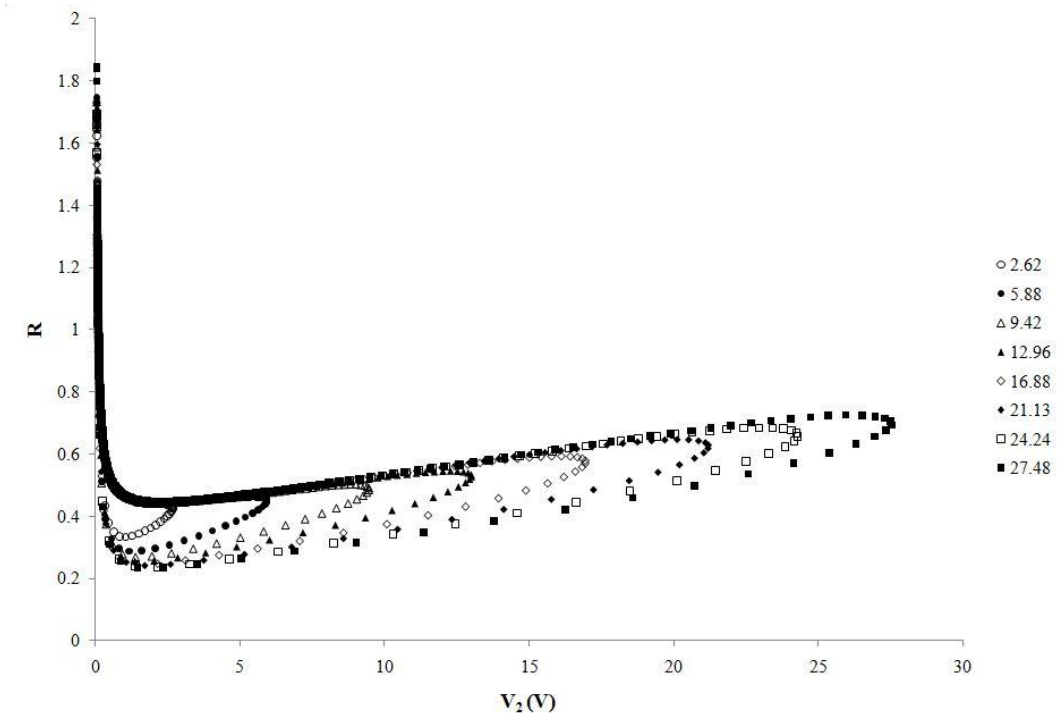

Figure 14. Chromatogram data for NBS-30 at various sample sizes. Maximum peak amplitude is indicated in the legend.

function of V_2. This is due to the increasing contribution of H_3^+ to V_3, and is exactly the effect described by Friedman (1953). The rate of increase in R is the H_3^+-factor. With no H_3^+-factor correction, chromatograms datasets appear as they do in Figure 14.

Three sets of chromatogram data, representing an analysis of the same sample of NBS-30, are show in Figure 15. Curve A has not been corrected for H_3^+. Curve B has been corrected for H_3^+ using the Isodat H_3^+-factor correction tool. Curve C has been corrected for H_3^+ using the method proposed in this thesis, which will be discussed in the following chapter. As a result of the behavior of these curves, Isodat can cause a bizarre increase in δD, following the observed nonlinear decrease, after a critical sample size threshold has been passed. This increase can be seen both in hydrocarbon data from Greule et al. (2008) (Figure 16), and more emphatically in benzoic acid data from this thesis (Figure 17). However, these effects can be eliminated by using the H_3^+ correction method proposed in this thesis, and by re-aligning the chromatographic peaks.

2.3.5. Chromatographic Separation

The geometry of the chromatogram data in figures 14 and 15, specifically the lobate form for data of a given sample size, is due to chromatographic separation of the isotopologues of molecular hydrogen. Additionally, because of its greater mass, the chromatographic peak generated by HD displays is slightly

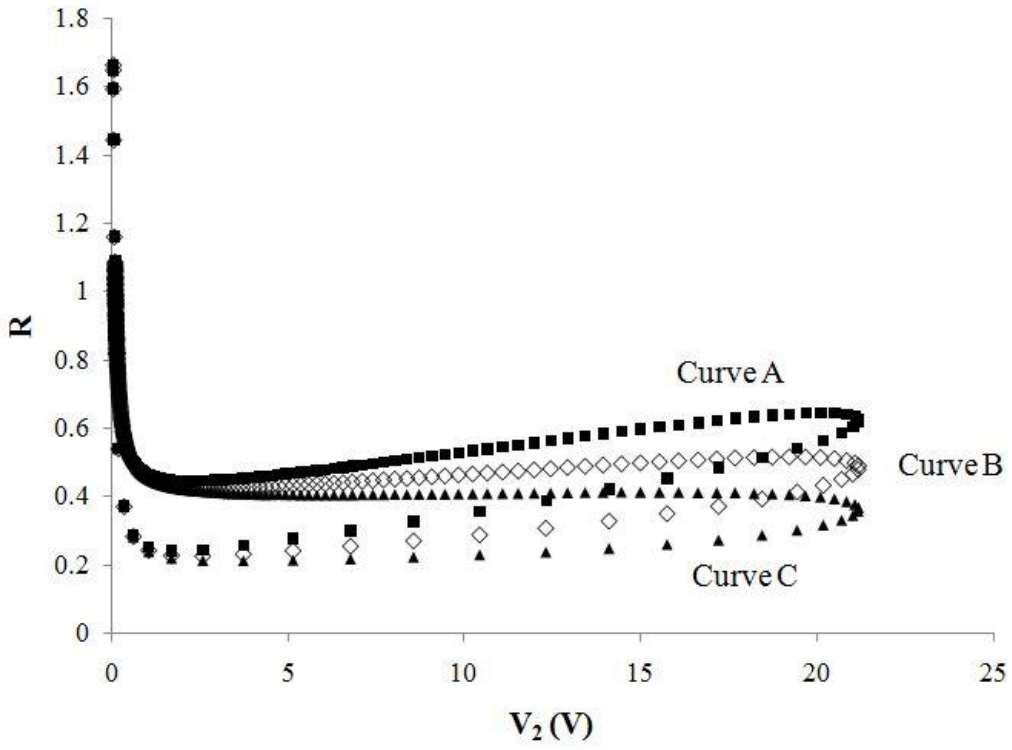

Figure 15. Chromatogram data for NBS-30 at a maximum peak amplitude of 21 V. The presence of an overall positive slope indicates that H_3^+ is contributing to V_3.

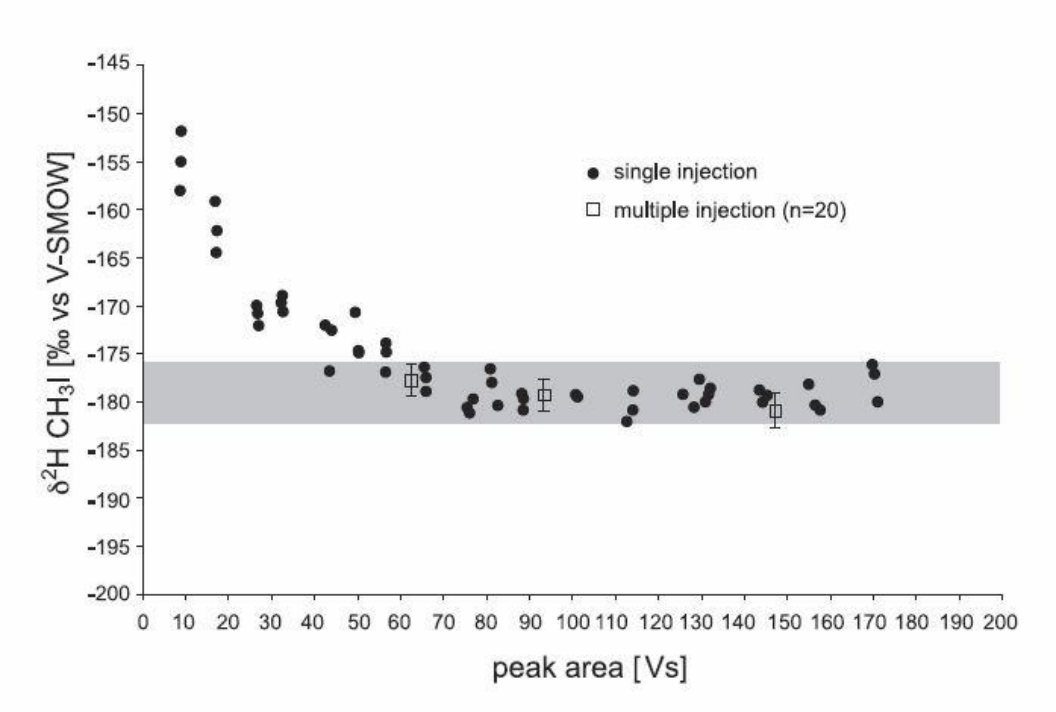

Figure 16. δD as a function of sample size (from Greule et al., 2008). After 160 Vs, δD begins to increase again.

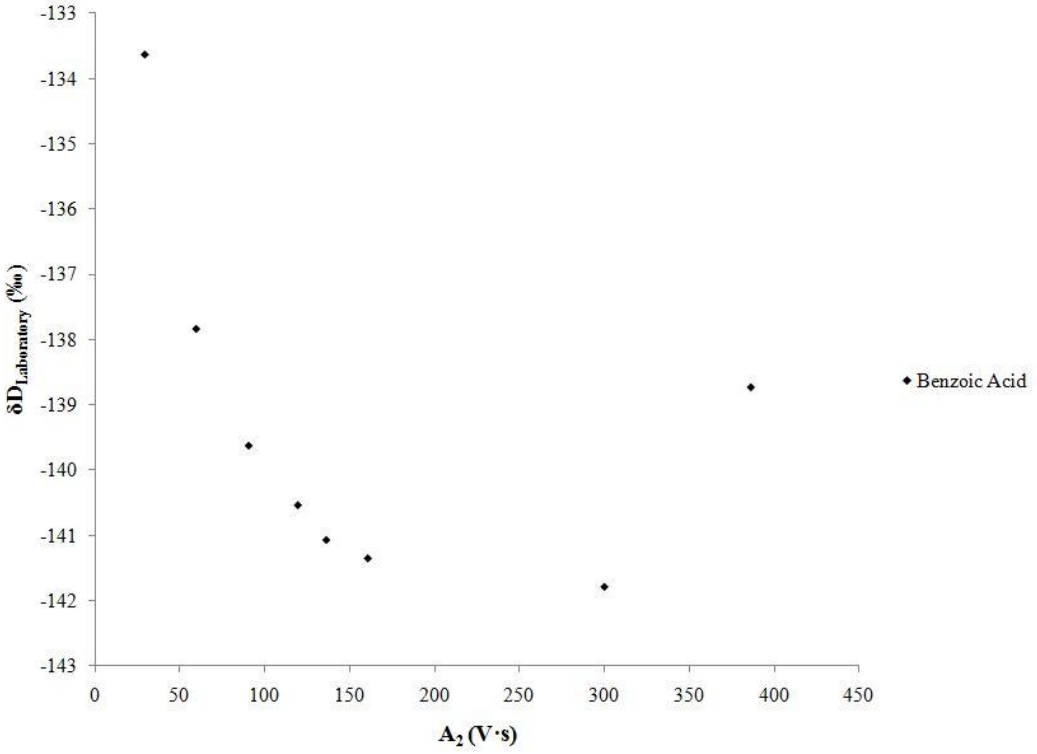

Figure 17. A more dramatic decrease and increase of δD than that observed in Greule et al. (2008).

broader than that generated by H_2. Figure 18 is comprised of chromatogram data derived from the analysis of NBS-30, with a maximum V_2 of 21.13 V. In this figure, V_3 is plotted as a function of V_2. The underside of the data represents the up-leg of the chromatographic peak as it approaches its maximum amplitude, while the upper side of the curve represents the down-leg of the chromatographic peak as it descends from the apex. Figure 19 is the accompanying graph of figure 18, in which R is plotted as a function of V_2. Likewise, in this figure, the underside of the curve represents the up-leg of the chromatographic peak and the upper side of the curve represents the down-leg of the chromatographic peak. In Figure 20, the contribution to V_3 from H_3^+ has been removed; following removal of H_3^+, background levels have been subtracted individually from each point. It is now possible to see that even with the contribution from H_3^+ eliminated and background levels removed, there is a factor which precludes a constant isotope ratio from being measured in GC-IRMS. This factor is the chromatographic separation of the isotopologues of hydrogen gas. The molecule H_2 arrives in the ion source seconds before the molecule HD. This separation manifests in a relatively low instantaneous isotope ratio throughout the up-leg of the chromatographic peak. In the same manner, the molecule HD continues to arrive in the ion source seconds after H_2 has been exhausted, resulting in a relatively high instantaneous isotope ratio throughout the down-leg of the chromatographic peak. When the data is shifted in order to align the apexes of the V_2 and V_3 chromatographic peaks, as they would without chromatographic separation, R

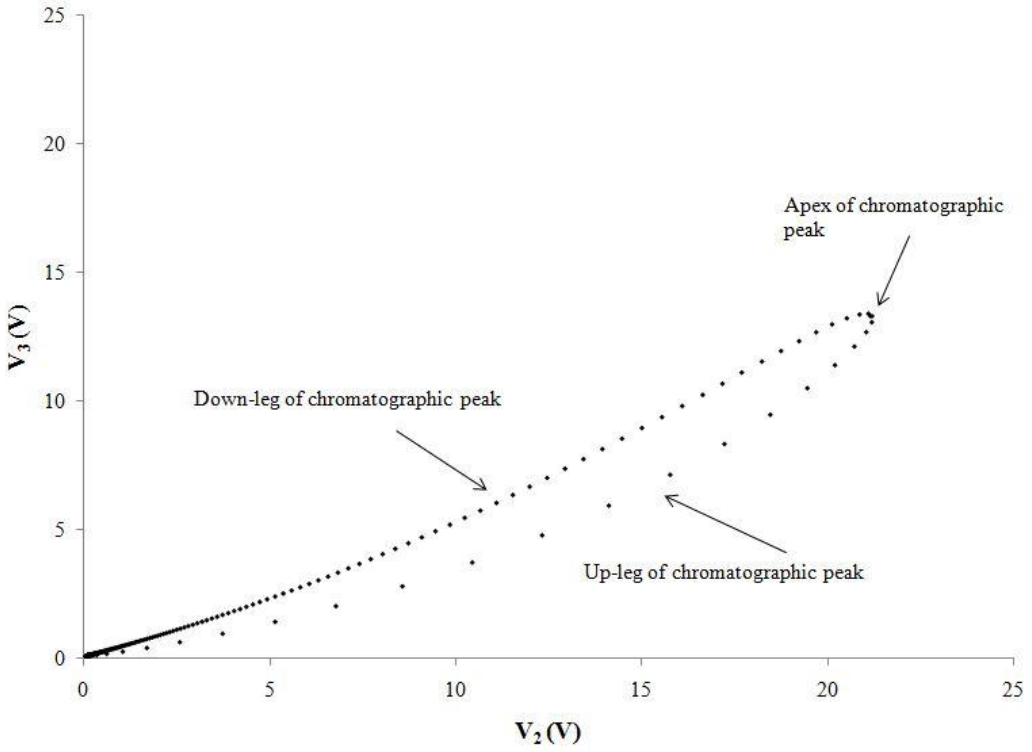

Figure 18. Chromatogram data from a chromatographic peak of NBS-30. V_3 is plotted as a function of V_2. The slight overall upward curve of the data indicates a contribution from H_3^+.

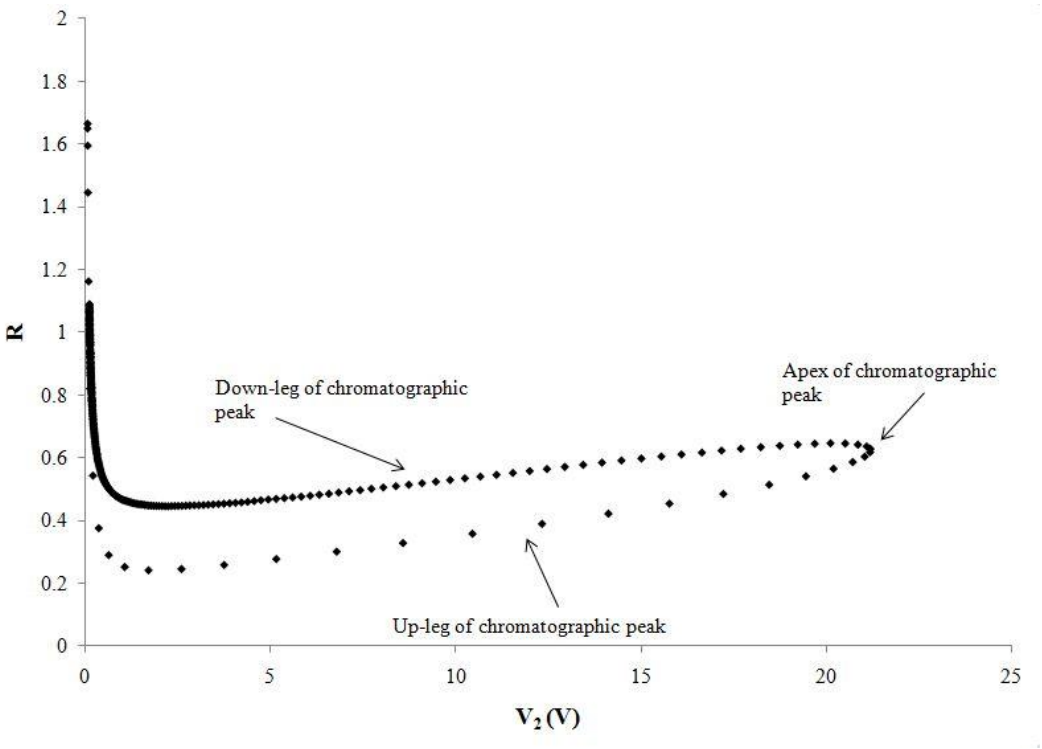

Figure 19. Chromatogram data from Figure 18. In this example, R is plotted as a function of V_2. The overall positive slope of the lobate section of the data indicates a contribution from H_3^+.

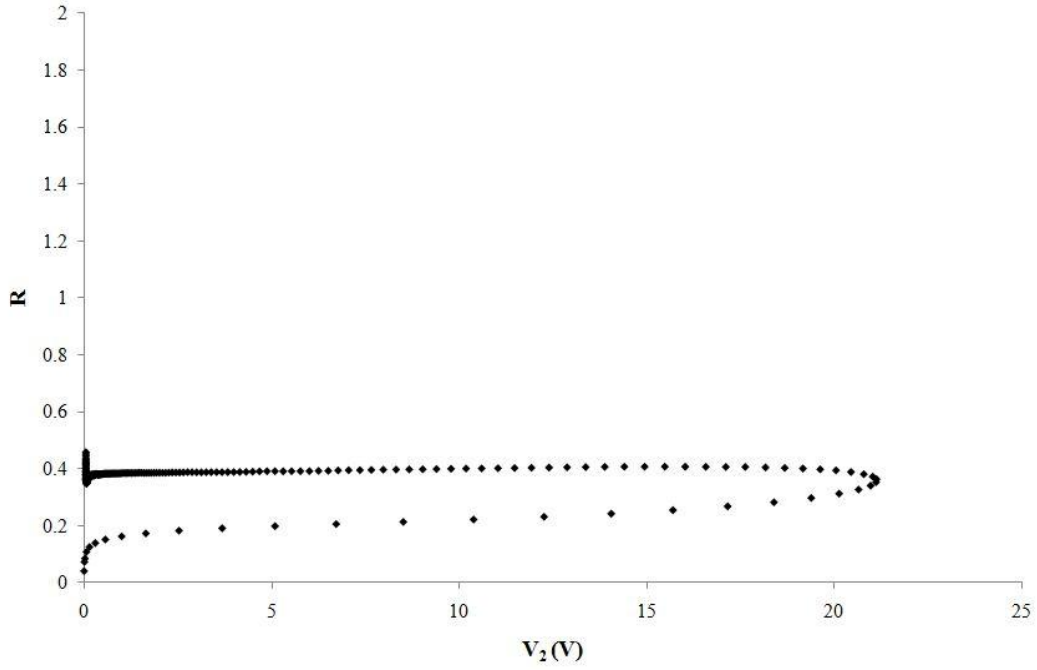

Figure 20. The instantaneous isotope ratio, R, plotted as a function of V_2, taken from chromatogram data of NBS-30. In this figure, the contribution from H_3^+ has been removed.

approaches a constant value (Figure 21). This is accomplished using spreadsheet software by manually shifting the data such that the maximum values of V_2 and V_3 occur at the same time. The outlying data points in Figure 21 are most likely due to poor resolution of the data, and broadening of the V_3 chromatographic peak.

2.3.6 Evaluation of Sharp et al. (2001)

As noted previously, Sharp et al. (2001) were the first to use a TC/EA coupled with a mass spectrometer to measure D/H in water liberated by flash heating in a GC-IRMS system. Sharp et al. (2001) implicitly indicated an undefined dependence of the observed value of δD on sample size. To counter the effects of sample size on δD, Sharp et al. (2001) manually adjusted the H_3^+-factor. The range of δD could vary drastically for different values of the H_3^+-factor, as in Figure 8. The data in this thesis suggest that Isodat underestimates the value of the H_3^+-factor by as much as half (Figure 15). The suggested H_3^+-factor given by Sharp et al. (2001) is slightly greater than that given by Isodat, but does not approach the correct value (Figure 15). Sharp et al. (2001) assumed that the changing partial pressure of hydrogen in the ion source during the course of an analysis hampered the ability of Isodat to correctly calculate the H_3^+-factor of the instrument. Sharp et al. (2001) therefore indirectly implicated Isodat as the cause of any sample size issues. However, Sharp et al. (2001) seem to have

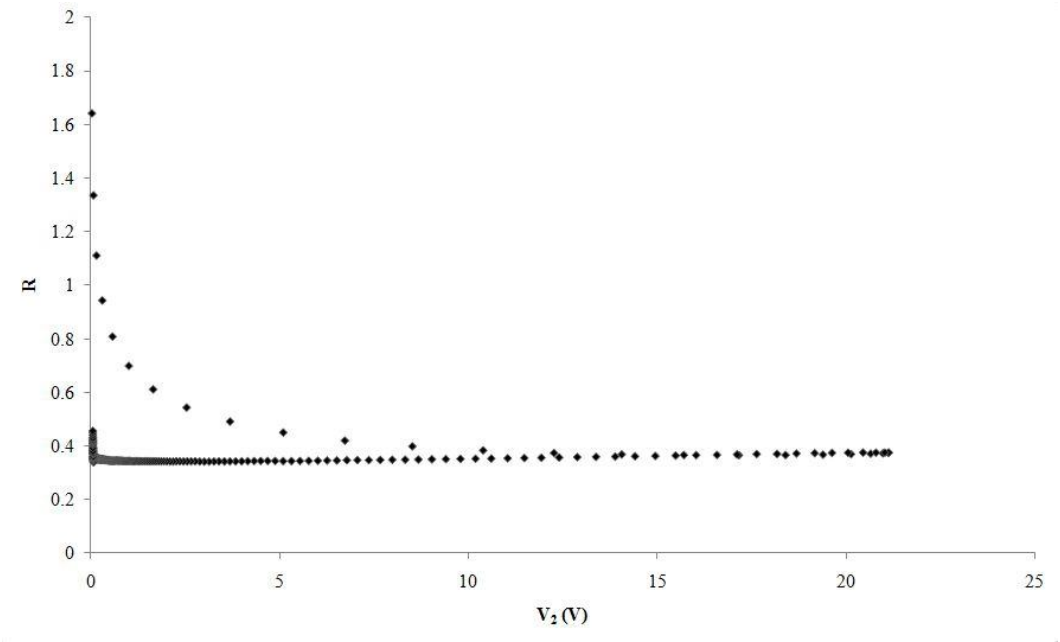

Figure 21. The instantaneous isotope ratio, R. The chromatographic peaks of V_2 and V_3 have been shifted such that the apexes intersect. Compare to Figures 19 and 20.

misunderstood both the H_3^+-factor itself as well as how the Isodat H_3^+-factor correction tool operates. Sharp et al. (2001) stated, "In continuous flow measurements, signal strength is continuously changing, meaning that the H_3^+-factor is also changing during acquisition of a single peak." This statement is incorrect. As can be inferred from Friedman (1953), the H_3^+-factor is the rate of H_3^+ production in the ion source of the mass spectrometer. It is entirely dependent upon the ion source parameters of the mass spectrometer, but is nonetheless extremely stable over time. During the course of a single measurement, the H_3^+-factor does not change. Rather, the contribution of H_3^+ to V_3 changes as V_2 changes, according to the value of the H_3^+-factor as defined by Friedman (1953). Sharp et al. (2001) go on to state, "…Isodat software is written to calculate a separate H_3^+-factor for each point along a peak, effectively integrating the H_3^+-factor over the entire dynamic peak (e.g. Sessions et al., 1999)." However, this claim is also incorrect. Isodat uses only one H_3^+-factor that must be either calculated prior to any analyses or inputted manually, as above, and applies that value to every datum along a chromatographic peak in its correction algorithm. Sharp et al. (2001) attribute both the design of the Isodat H_3^+-factor tool as well as their assumption about the functionality of the tool to Sessions et al. (1999). However, Sessions et al. (1999) clearly state that their program calculates the H_3^+-factor as that value which minimizes the absolute error of δD in 15 chromatographic peaks of a known n-alkane. In the calculation method designed by Sessions et al. (1999), one of the 15 chromatographic peaks is designated as

the reference peak and assigned an arbitrary δD value by the experimenter. The H_3^+-factor that minimizes the absolute error in the δD-values of the remaining peaks is selected through an iterative calculation process. The program designed by Sessions et al. (1999) then corrects every integrated point along subsequent chromatographic peaks using that value. Although the program designed by Sessions et al. (1999) is applying a single value for the H_3^+-factor over a range of pressures to minimize the absolute error between measurements, it does not represent an actual measurement of the H_3^+-factor of the instrument as defined by Friedman (1953), nor is it recalculated in real time during a measurement as claimed by Sharp et al. (2001). It is evident that this use of the H_3^+-factor tool by Sharp et al. (2001) is both ad hoc and inappropriate, as it neither identifies the source of the observed sample size issue nor does it allow the production of reproducible data in every case.

While attempting to replicate the method of data reduction used by Sharp et al. (2001), several difficulties were encountered. Sharp et al. (2001) manually adjust the value of the H_3^+-factor used by the Isodat tool to correct for the contribution of H_3^+ to the mass-3 signal. In doing this, Sharp et al. (2001) have attempted to apply the value which results in the least correlation between sample size and δD. To do this, Sharp et al. (2001) iterate a number of values for the H_3^+-factor until they reach a value that produces both a sufficiently low standard deviation in δD for a given substance as well as an apparent lack of correlation as determined by an R^2 value approaching zero when $\delta D_{Laboratory}$ is plotted as a

function of V_2. While it is possible that this is an effective way to correct for the contribution of H_3^+ to V_3, it is also possible to introduce significant error. Ultimately, it falls to the experimenter to reevaluate all data over a series of H_3^+-factors rather than performing a direct measurement of the rate of H_3^+ production in the ion source.

Selection bias readily occurs when using the method described by Sharp et al. (2001). In Figure 22, data for NBS-30, the same isotopic reference material used by Sharp et al. (2001) in their illustration of the H_3^+-factor as well as in previous figures of this thesis, is presented. In this figure, an H_3^+-factor of 6.00 has been manually entered into the Isodat H_3^+-factor correction tool. This H_3^+-factor reduces the standard deviation of δD for the given sample sizes of NBS-30 to approximately 1.85‰ – within the accepted external precision of D/H measured by conventional means, and better than most of the data in Sharp et al. (2001). Moreover, it produces only a weak correlation between δD and V_2. In short, this H_3^+-factor value appears to be acceptable using the method of Sharp et al. (2001) over a larger range of the mass spectrometer's capabilities than is attempted in Sharp et al. (2001). When a larger range of data is considered (Figure 23), the method fails. The result is a standard deviation of 6.27‰, and a strong, positive correlation between V_2 and δD. If this H_3^+-factor is applied to all of the data based upon the behavior of a single standard over a small range of sample sizes, as in Sharp et al. (2001), significant error is likely as there is no evidence to suggest that all substances analyzed will behave in the same manner.

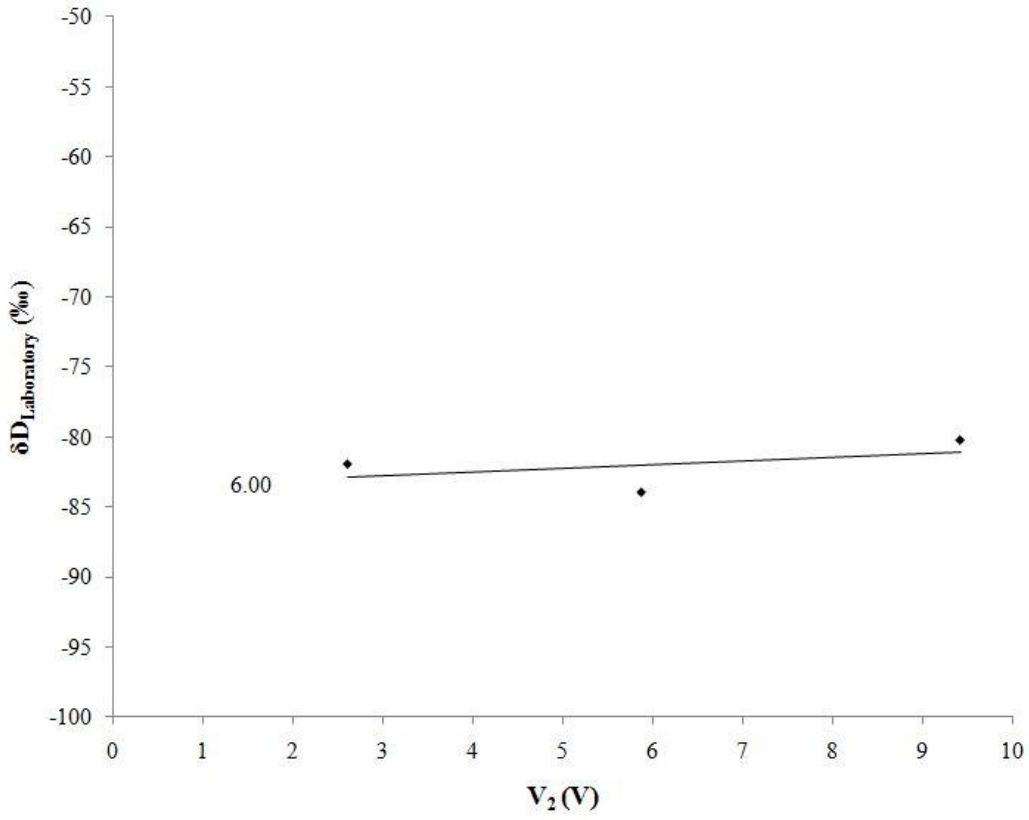

Figure 22. Data correction using the method described by Sharp et al. (2001). This figure illustrates a weak correlation between the isotope ratio and sample size in NBS-30.

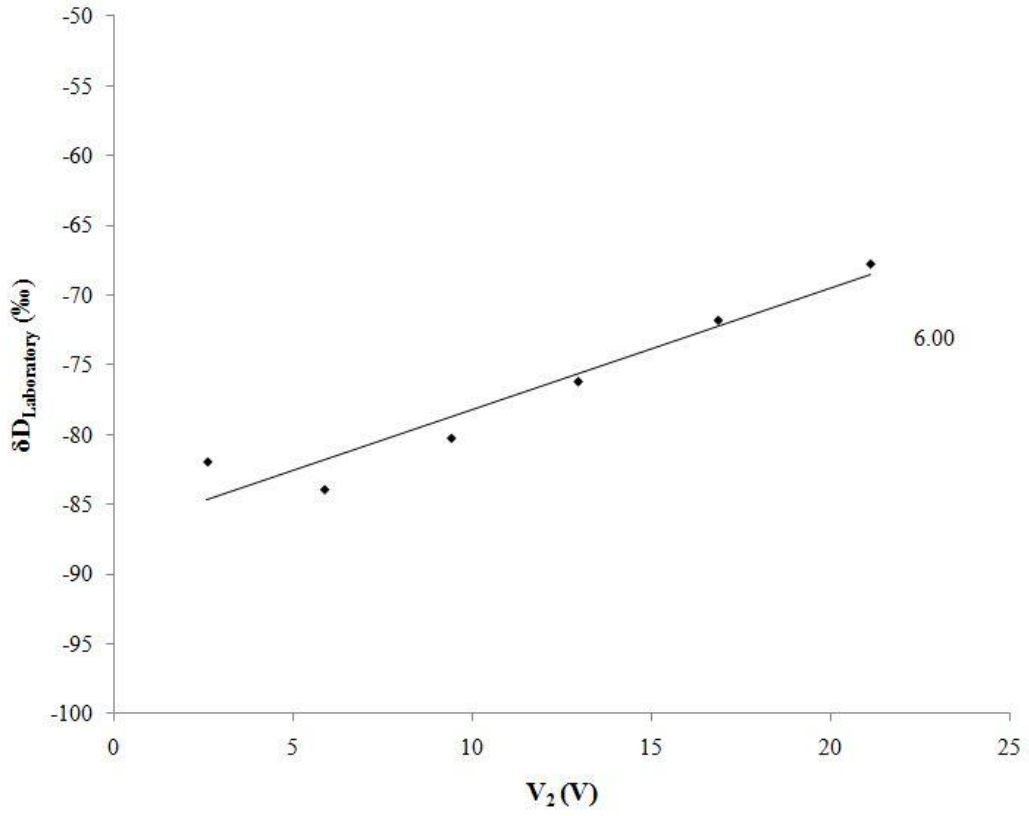

Figure 23. The same dataset from which Figure 22 is drawn. In this case, the data range has been extended to approximately 10 times that used by Sharp et al. (2001).

Figure 24 illustrates this. In keeping with the data from Figure 22, the same H_3^+-factor has been applied to silicified basalt 125. The result is a poor precision measurement and a δD that overlaps with the value for NBS-30. The correct value of silicified basalt 125, at -58‰ (VSMOW), is nearly 10‰ more positive than the accepted value of NBS-30. While the value determined using the analytical method of Sharp et al. (2001), overlaps with that of NBS-30.

Sharp et al. (2001) go on to state that this manual adjustment of the H_3^+-factor is in good agreement with the conventional method of measurement as described by Friedman (1953). This statement is incorrect. When the H_3^+-factor is determined by the method described in Friedman (1953), the value is commonly close to double that determined by the method described by Sharp et al. (2001). When the H_3^+-factor, determined according to the method described by Friedman (1953), is manually entered into Isodat, the result is a strongly correlated relationship between δD and sample size on the order of -25‰ per Volt of signal (Figure 25). This is something that could be corrected, provided the mechanism is understood and all substances behave identically. However, the slope does vary by several percent depending upon sample composition. The result being that the relative displacement between known and unknown substances can vary and even reverse, leading to incorrect δD-values.

Because of the issues outlined above, in order to determine the correct δ-value of an unknown substance, one would have to know the relative relationship between an unknown and a standard. It is also impossible to extrapolate to zero-

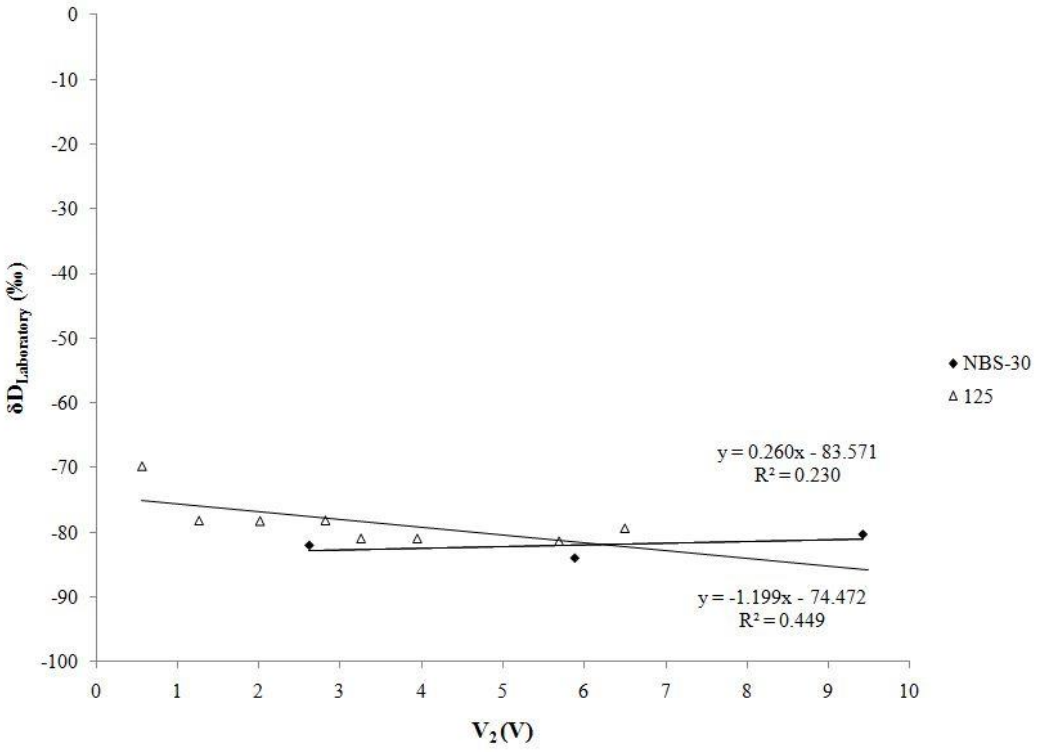

Figure 24. Error introduced by overcorrection, using an iterative, manually entered value for the Isodat H_3^+-factor correction tool.

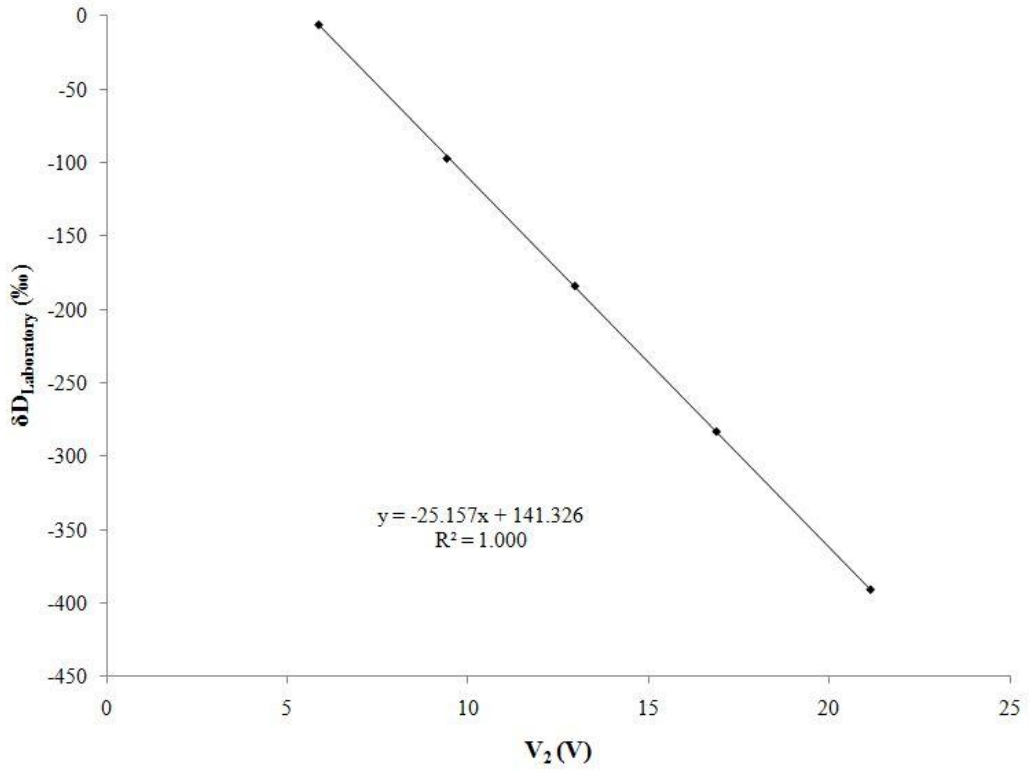

Figure 25. The H_3^+-factor has been calculated according to the method described by Friedman et al. (1953), and referred to by Sharp et al. (2001). The isotope ratio for NBS-30 is strongly correlated with sample size.

pressure or zero-voltage, as Friedman (1953) did while using the method outlined by Sharp et al. (2001), because the instantaneous isotope ratio is never assessed.

A further issue arises when one considers the effects of memory on the system. A small but persistent memory effect is present in pyrolysis facilitated GC-IRMS. Sharp et al. (2001) reported a memory effect, but only with liquid samples and therefore attributed it to the heated septum or needles used during the injection of the liquid. However, data collected here suggests a memory effect in the analysis of solid samples. If Sharp et al. (2001) did not correct or remove the first several analyses following a change in sample composition they would have been correcting for any memory effect while attempting to correct the H_3^+ contribution to V_3. Take for example, the determination of the H_3^+-factor using NBS-30 by the method outlined by Sharp et al. (2001). If NBS-22, with a value of -118.5‰ (VSMOW) had been analyzed immediately prior to it, given the same H_3^+-factor, the first few analyses would appear to have a significantly depleted isotope ratio. As a result, the experimenter would choose a different iterative value for the H_3^+-factor. The data in Figures 22, 23, and 24 was produced without regard for memory effects to illustrate this very point. In Figure 24, benzoic acid at -119‰ (VSMOW) had been analyzed just prior to NBS-30, whereas 125 had been analyzed immediately following NBS-30. The result is an overcorrection for the NBS-30 data that gives the weak correlation observed for NBS-30 and the relatively strong negative correlation observed in 125.

The final step in the data reduction method described in Sharp et al. (2001) and Sharp (2006) is the correction of isotopic compression and shifting caused by the calibration of an instrument. In this step, also used by Eiler and Kitchen (2001), the laboratory derived δ-value of a substance is plotted as a function of the accepted δ-value of the same substance on the proper scale. This requires that two or more laboratory standards or NIST standards be analyzed along with any unknowns for a given series of analyses. For example, NBS-22, NBS-30 and IAEA CH7 may be analyzed along with any unknowns. The accepted δ-values of the standards are then plotted as a function of the observed values. The resulting curve is then applied to all measured unknowns to correct for the error introduced by the calibration of the instrument. As in Abruzzese et al. (2005), this final step is a prudent correction, provided that any prior steps in the analysis and data reduction method are valid.

2.3.7 Evaluation of Abruzzese et al. (2005)

C.P. Chamberlain provided several Excel spreadsheets illustrating the data reduction method used in Abruzzese et al. (2005) and in Hren et al. (2009) (personal communication). In both Abruzzese et al. (2005) and Hren et al. (2009), the same methods of sample preparation, analysis, H_3^+-factor correction, and final data reduction are used (Chamberlain, personal communication). In these studies, solid samples were crushed in a shatterbox using a tungsten-carbide

puck. All material that passed 175 US Standard Mesh Sieve was kept for analysis. Powders were chemically treated to remove carbonate and organic material using HCl and household bleach. Sample powders were then loaded into silver boats and dried in a vacuum oven at 80°C for four hours to remove surface water. Samples were then rapidly transferred to an autosampler where they were flushed with helium prior to analysis. The previous two steps are ambiguous because it is not indicated whether the 'silver boats' refer to the silver capsules in which samples are contained when introduced to the TC/EA, or if they are simply containers from which the silver capsules are filled. Regardless, any exposure to atmosphere causes immediate condensation of exchangeable water that tends to be isotopically depleted. In substances with high surface area to volume ratios, such as powdered chert, this exchangeable surface water can make up more than 0.2 wt%H_20 (Knauth and Epstein, 1982). Presumably, this adsorption of water will occur to some degrees on any hygroscopic material with a sufficiently high surface area to volume ratio, such as the material size accepted for analysis in Abruzzese et al. (2005) and Hren et al. (2009).

Chamberlain explained that in both Abruzzese et al. (2005) and Hren et al. (2009), the H_3^+-factor is determined prior to any analyses by letting 10 or more pulses of a hydrogen monitoring gas in to the ion source via the open-split, while bypassing the TC/EA entirely (Personal Communication, January 17, 2009). The pulses of hydrogen gas are introduced in varying pressures, such that the resulting chromatographic peaks are all of different amplitude and area. The authors then

use the Isodat H_3^+-factor correction tool to evaluate the data and calculate the H_3^+-factor of the instrument. As stated above, the Isodat H_3^+-factor correction tool employs an iterative calculation that reduces the total error in δD-value over the given range in peak area, similar to the program designed by Sessions et al. (1999). That H_3^+-factor is then applied to all subsequent analyses. Next, five samples of a working standard, prepared at various sizes, are analyzed. The instrument derived isotope ratio, $\delta D_{Laboratory}$ is then plotted as a function of sample size – in this case the area under the chromatographic peak, A_2 (V·s). The resulting data is fit to a curve of the form $y = -a\ln(x) + b$. See Figure 26 for data provided by M. Hren, in which data from a working standard, a kaolinite labeled KGa2, is presented that exhibits this relationship (personal communication). Abruzzese et al. (2005) and Hren et al. (2009) then assume that this curve is replicated, with an offset depending upon δD-value, by all subsequent analyses. C. Page Chamberlain attributed this curve to some sort of kinetic fractionation, "…[Curve shape] is not related to H3 factor, but is likely something physical, either related to fractionation at an open split, loss of gas somewhere in the reaction column…," (Personal Communication, January 17, 2009). To correct for this nonlinearity, Abruzzese et al. (2005) 'normalize' their data to an arbitrary value of A_2 that falls within the minimum and maximum of their calibration curve. In short, assuming that all of their data plots on a curve of the same form, they calculate the difference between the best fit curve at the value of A_2 of an unknown and the desired normalizing value. They then subtract this

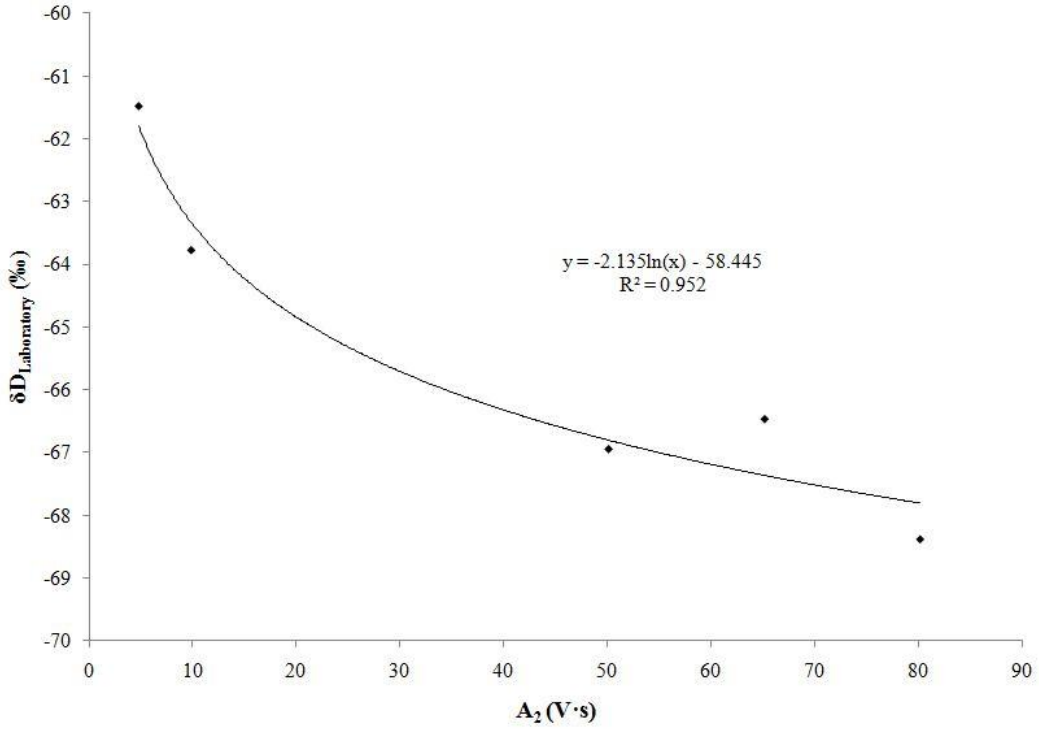

Figure 26. Data provided by M. Hren (Personal Communication, April 26, 2010). δD is shown as a function of sample size for the laboratory standard, Kga2, a kaolinite.

value from the $\delta D_{Laboratory}$-value of the data, in effect straightening their curve while retaining the natural distribution of their data. Following the establishment of this calibration curve, analyses of unknowns and isotopic standards are made, occasionally with one or two replicate analyses for an unknown, and without regard to memory effects. Were the mechanisms of this nonlinearity perfectly understood and the logarithmic curve constant for all materials, the empirical correction suggested above would suffice. However, these conditions are not satisfied.

The nonlinear dependence of δD on sample size was attributed to kinetic fractionation that was supposedly a characteristic of all pyrolysis facilitated GC-IRMS systems (Chamberlain, personal communication). If this were the case, the resulting curve would be of identical shape but with a different intercept for any substance measured on a given day, assuming an identical H_3^+-factor and source settings. However, this has not been observed in this thesis. Data collected in this thesis indicates that a given substance generates a unique curve when the method used by Abruzzese et al. (2005) and Hren et al. (2009) is employed. Moreover, it is possible for these curves to intersect (Figure 27). If this type of calibration curve is created for every substance, depending upon the normalizing value the resulting δ-values of unknowns could vary significantly (Table 1). In the case above, the two unknowns, benzoic acid and 125, vary by nearly 10‰. Intersections appear to occur more frequently at low peak areas – particularly at the peak area values the vast majority of chert samples analyzed in Hren et al.

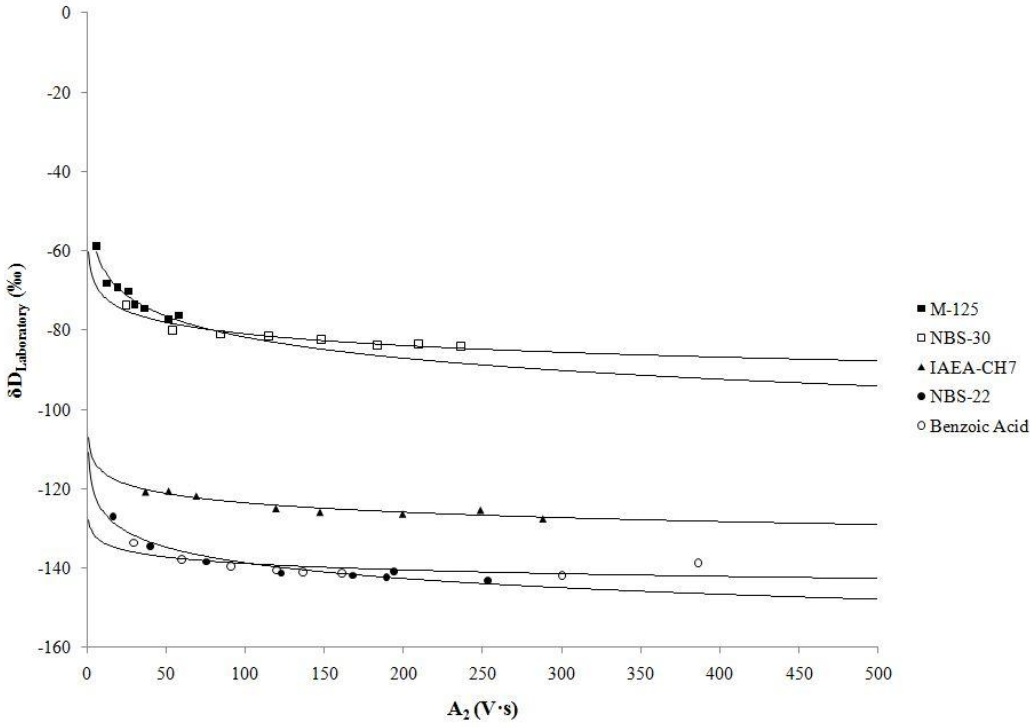

Figure 27. $\delta D_{Laboratory}$ as a function of sample size, A_2. In this figure, the data are shown to intersect.

Table 1. Variation in data using the method of Abruzzese et al. (2005) and Hren et al. (2009)

Normalized to 5 Vs		
Composition	δD (‰ VSMOW)	2σ
125	-56	2.40
Benzoic Acid	-123	3.35
IAEA CH7	-107	1.48
NBS-22	-114	2.20
NBS-30	-65	1.71

Normalized to 50 Vs		
Composition	δD (‰ VSMOW)	2σ
125	-63	2.41
Benzoic Acid	-119	3.36
IAEA CH7	-104	1.49
NBS-22	-117	2.21
NBS-30	-65	1.72

Normalized to 100 Vs		
Composition	δD (‰ VSMOW)	2σ
125	-66	2.34
Benzoic Acid	-117	3.26
IAEA CH7	-103	1.45
NBS-22	-116	2.14
NBS-30	-65	1.67

(2009) fall within. When this occurs, the correct normalizing value of A_2 cannot be determined, because the relative difference in δD between an unknown and a standard is, by definition, unknown. This method of analysis and data reduction seems to exhibit circular reasoning – that in order to properly identify the correct δ-value of an unknown substance, one must already know both the relative difference in D/H between the substance and a standard as well as the absolute difference in order to make an accurate measurement. The final step in the data reduction is the correction for compression and offset due to instrument calibration as described in Sharp (2007).

The method of data reduction used by Abruzzese et al. (2005) and Hren et al. (2009) incorrectly identifies kinetic fractionation as the cause of the δ-value dependence on sample size, and is particularly prone to selection bias: the shape of the curve generated by plotting observed δD as a function of A_2 depends upon the range of sample sizes selected for analysis. If one chooses samples representing a range of particularly large sample sizes, one will, for the most part, obtain a relatively gentle curve. For small values of peak area, one will obtain a very irregular curve. For these reasons, this method of data reduction is largely inaccurate and cumbersome. Data derived using this method of analysis and data reduction should be thoroughly reevaluated.

2.4 Proposed Method

2.4.1. Calculation of δD

Based upon the issues identified in Isodat, inconsistencies and error in the method of analysis described by Sharp et al. (2001), and the high probability of generating inaccurate data in the method used by Abruzzese et al. (2005) and Hren et al. (2009), it is clear that a new method of analysis and data reduction is required. In all three of the above cases, whether one accepts the raw data outputted by Isodat, manually adjusts the H_3^+-factor after Sharp et al. (2001), or accepts the H_3^+-factor given by Isodat and assumes and then corrects for kinetic fractionation or linearity as in Abruzzese et al. (2005) and Hren et al. (2009), the contribution to V_3 by H_3^+ is underestimated and therefore improperly corrected. The question of whether the H_3^+-factor may be correctly measured in pyrolysis facilitated GC-IRMS immediately arises. As was shown in Figure 15 and Figure 20, it is possible to remove the contribution due to H_3^+ by a point-wise correction to a single chromatogram – confirmation of a portion of the untested method described by Sessions et al. (2001a). However, due to the effects of chromatographic separation, it is apparently impossible to derive the H_3^+-factor directly from a dataset extracted from a single chromatographic peak. However, by taking a more macroscopic view and observing the similarities of

chromatogram datasets from a series of chromatographic peaks, it is possible to correctly identify the H_3^+-factor.

In figure 28, the same data that comprised figure 14 is shown, but with a best fit line through the values that represent the apexes of the chromatographic peaks; the maximum value of V_2. The chromatogram data is drawn from several chromatographic peaks of NBS-30 at different sample sizes analyzed consecutively. There are three factors that cause the variable instantaneous isotope ratio along a chromatographic peak: the contribution of H_3^+ to V_3, contribution to the total values of both V_2 and V_3 by constant background levels, and offset of the chromatographic peaks due to chromatography (Figures 18 through 21). Based upon the behavior of the chromatogram data, it is apparent that if analogous points on several chromatographic peaks are selected, e.g. the apex of the peak, both the background levels and the extent of chromatographic offset will be constant at those points. The only difference between those points are the values of V_2 and V_3. Because the values of V_2 are different, the contribution of H_3^+ to V_3 must be different. Therefore, the H_3^+-factor can be correctly calculated by comparing the values of V_2 and V_3 at the apexes of several chromatographic peaks of varying size for a given sample composition.

Figure 29 shows V_3 as a function of V_2 of the maximum peak amplitudes of samples of NBS-30 at varying sizes. As predicted by Friedman (1953), the equation best representing the data is a second order polynomial. In other words, as V_2 increases, V_3 increases at a rate greater than would be possible were there no

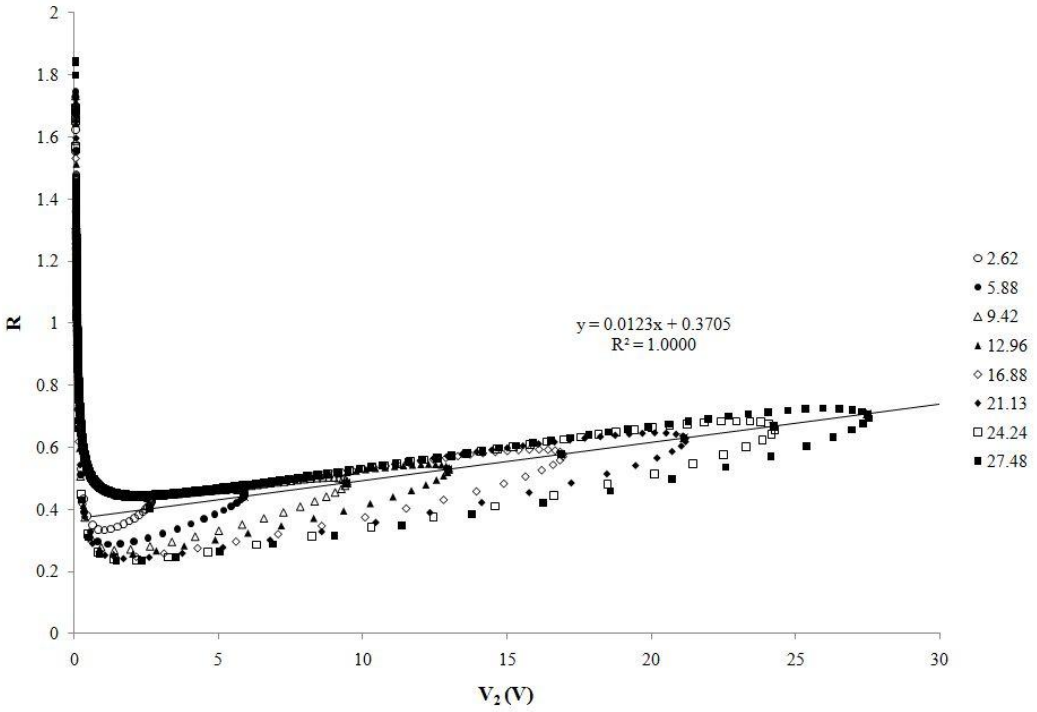

Figure 28. Reproduction of Figure 14, with a best fit line plotted through the maximum values of V_2 for each chromatographic peak. The slope of the curve is H_3^+-factor.

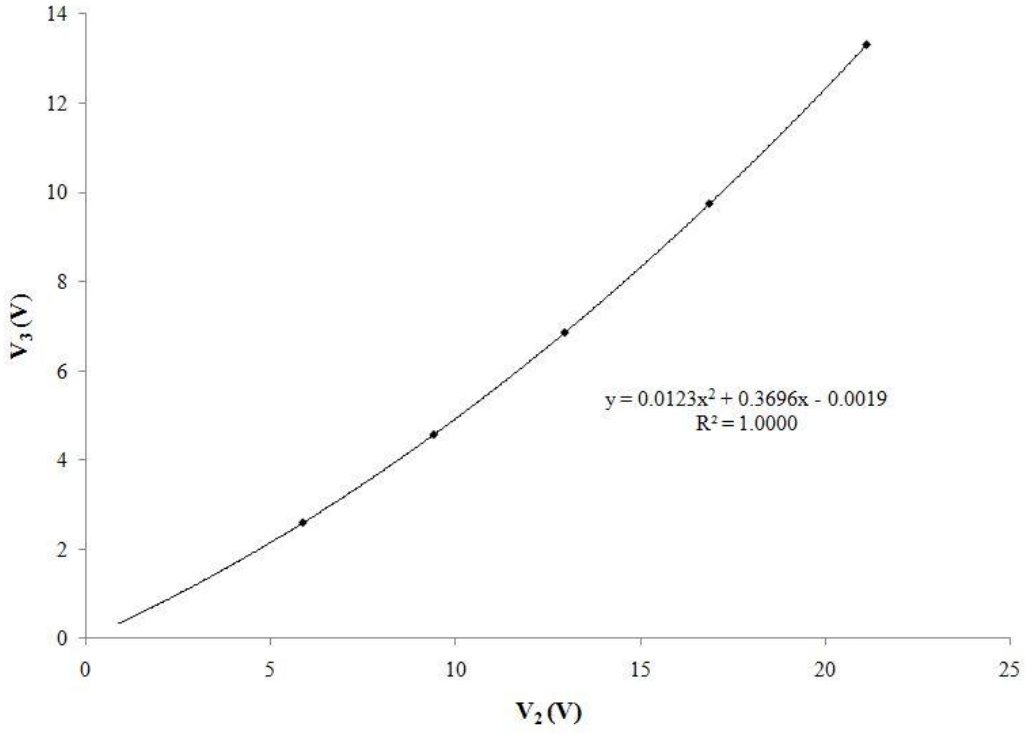

Figure 29. V_3 as a function of V_2 for NBS-30 (same data as Figures 14 and 29). The nonlinear nature of the curve is due to contributions from H_3^+.

contribution to V_3 by H_3^+. Figure 30 further illustrates this, as R increases at a constant rate. Were there no contribution to V_3 by increasing levels of H_3^+, R would be constant. The data is best described by the equation $R^* = kV_2 + R$. The slope of the best-fit line is the H_3^+-factor. Figure 31 shows additional data from the NIST standards IAEA-CH7 and NBS-22, analyzed on the same day as NBS-30. The best-fit lines for IAEA CH7 and NBS-22 also indicate an H_3^+-factor of 0.0123 V^{-1}, and perfect correlation at values of $R^2 = 1.0000$. Both the stability of the H_3^+-factor and the utility of this method of calculation have been confirmed exhaustively.

After having identified the H_3^+-factor for a given set of ion source parameters, the corrected value of R for unknown samples may be determined by solving $R = R^* - kV_2$, where R is the true isotope ratio, R^* is the observed isotope ratio, k is the H_3^+-factor and V_2 is the mass-2 signal voltage. When R has been calculated for two or more laboratory or NIST standards of known δD, it is possible to convert R to δD values. This is accomplished by plotting the accepted value of δD as a function of R (Figure 32). The value of δD for unknowns can be determined by solving the equation representing the best-fit line for δD.

In practice, approximately 8 analyses of a laboratory or NIST standard at various sample sizes must be analyzed sequentially in order to determine the H_3^+-factor. It is recommended that benzoic acid be used in the calculation of the H_3^+-factor as a large range of benzoic acid data is also necessary to determine the water content of unknowns. The first three analyses must be excluded from the

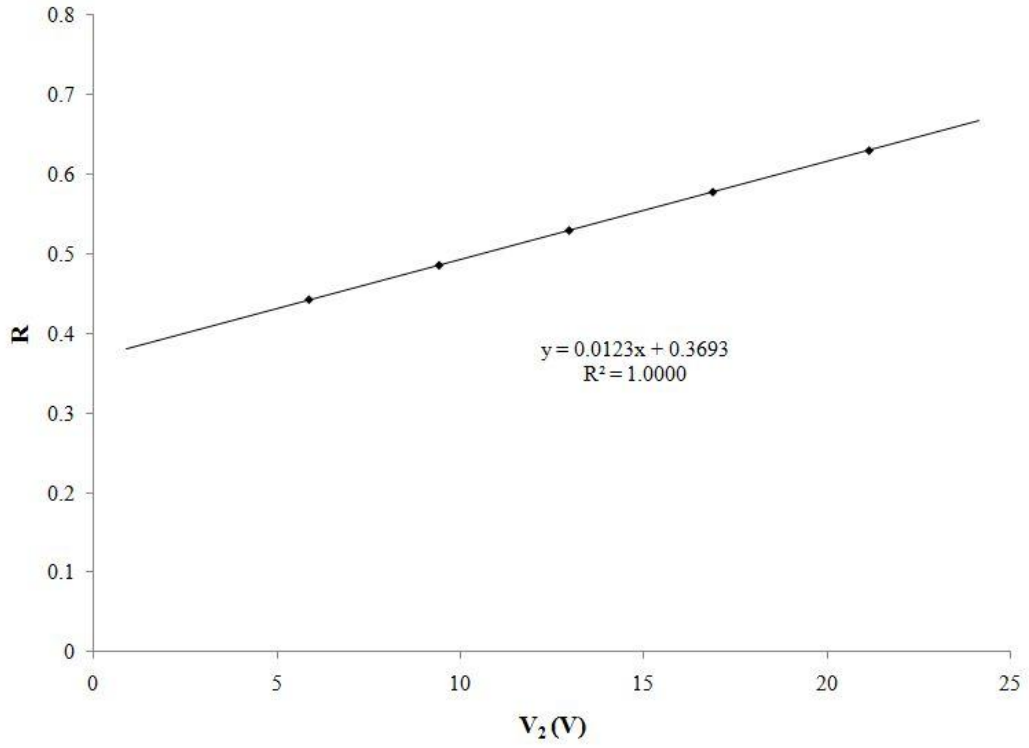

Figure 30. Data from Figure 29. The instantaneous isotope ratio, R, calculated from the apex of the chromatographic peak, is plotted as a function of V_2. The slope of the best fit line is the H_3^+-factor.

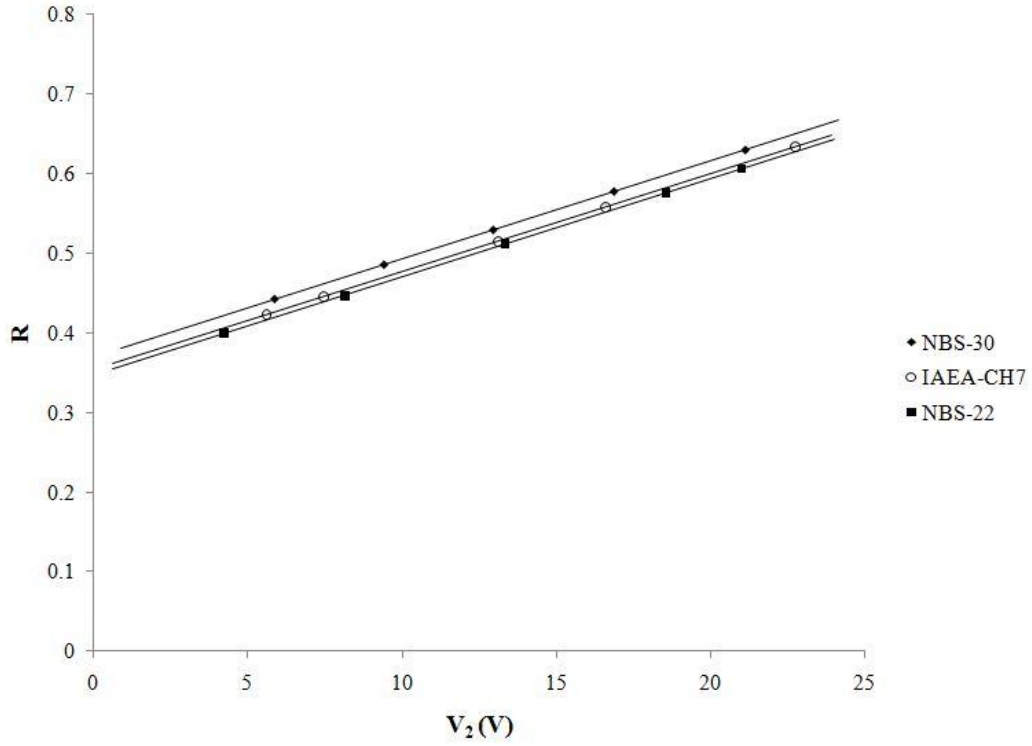

Figure 31. R as a function of V_2 for IAEA CH7, NBS-22 and NBS-30. The best fit lines possess the same slope and $R^2 = 1.0000$.

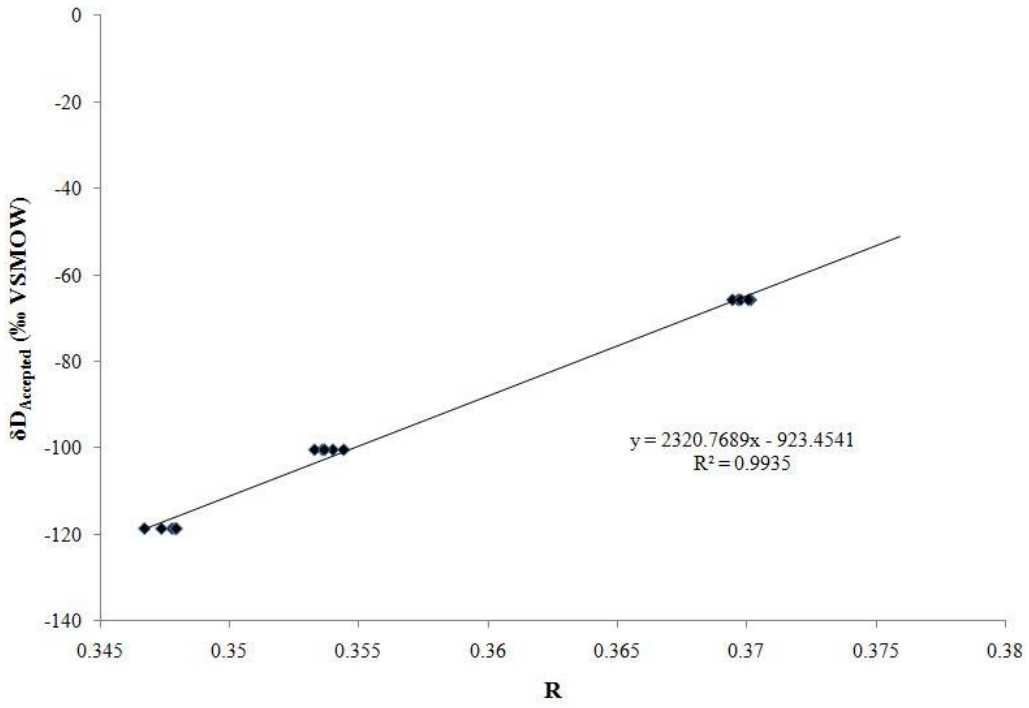

Figure 32. $\delta D_{Accepted}$ as a function of R. The accepted δD values for IAEA CH7, NBS-22, and NBS-30 are -100.3‰, -118.5‰, and -65.7‰ VSMOW, respectively.

H_3^+-factor calculation as they may be affected by memory. After the H_3^+-factor has been determined, unknowns should be bracketed by standards. Again, because the first three analyses of a new sample composition may be prone to memory effects, at least four samples of a standard or unknown must be analyzed sequentially in order to obtain an accurate and precise measurement. If greater precision through multiple measurements is required, a longer sequence of a standard or unknown may be analyzed.

2.4.2. Calculation of Hydrogen Content

The weight percent hydrogen or water can be determined with great accuracy and precision in GC-IRMS systems because the production of hydrogen gas during the pyrolysis step is quantitative. In order to accurately assess the weight percent hydrogen or water in an unknown, a calibration curve measuring the signal yield of benzoic acid must be compiled. Figure 33 illustrates the yield or calibration curve for benzoic acid. Benzoic acid contains approximately 5 wt%H. This known wt% is used as a reference for unknowns. Figure 34 illustrates the relative difference in yield between benzoic acid and the NIST standards Pef-1, NBS-22 and NBS-30. The Thermo Finnigan TC/EA Operation Manual indicates that $\mathrm{wt\%H} = \mathrm{k} \times \frac{\mathrm{A_2}}{\mathrm{Amount}}$, where $\mathrm{k} = \mathrm{wt\%H_{C_7H_6O_2}} \times \frac{\mathrm{Amount}}{\mathrm{A_2}}$. This is an effective calculation except that k does vary slightly depending upon sample size. The value of k varies by approximately 10% over the range of the

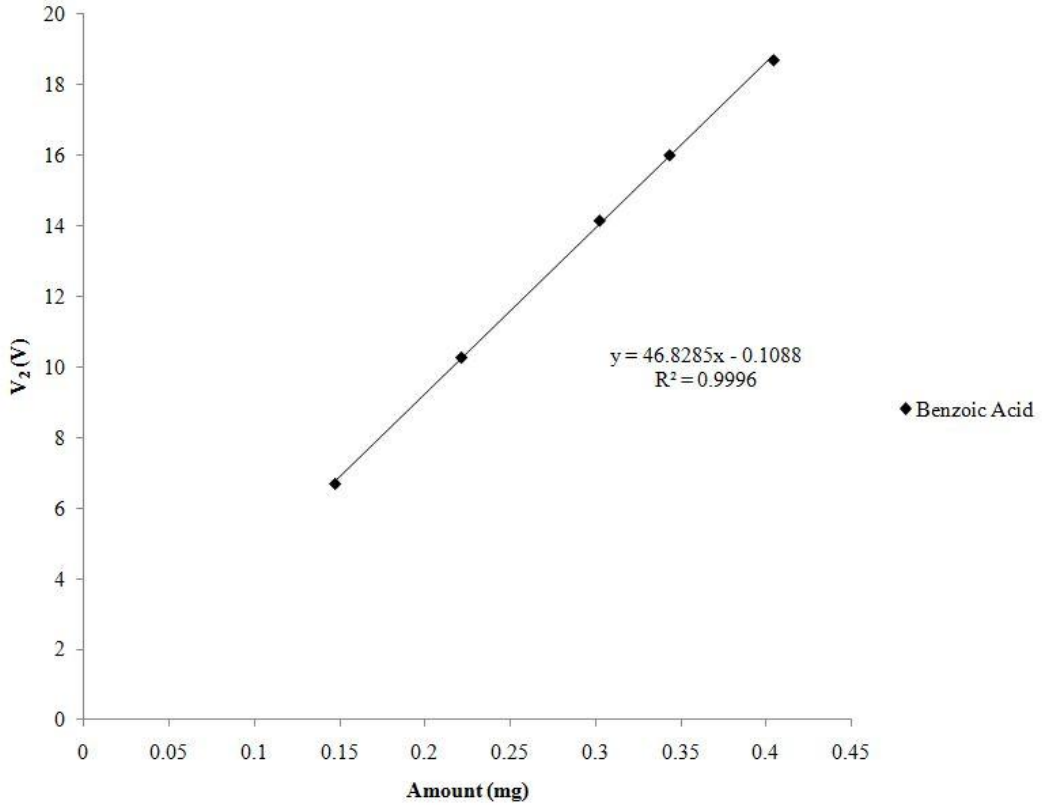

Figure 33. Calibration curve for benzoic acid, used to calculate weight percent hydrogen and water in unknown samples and standards. V_2 is shown as a function of sample weight (mg).

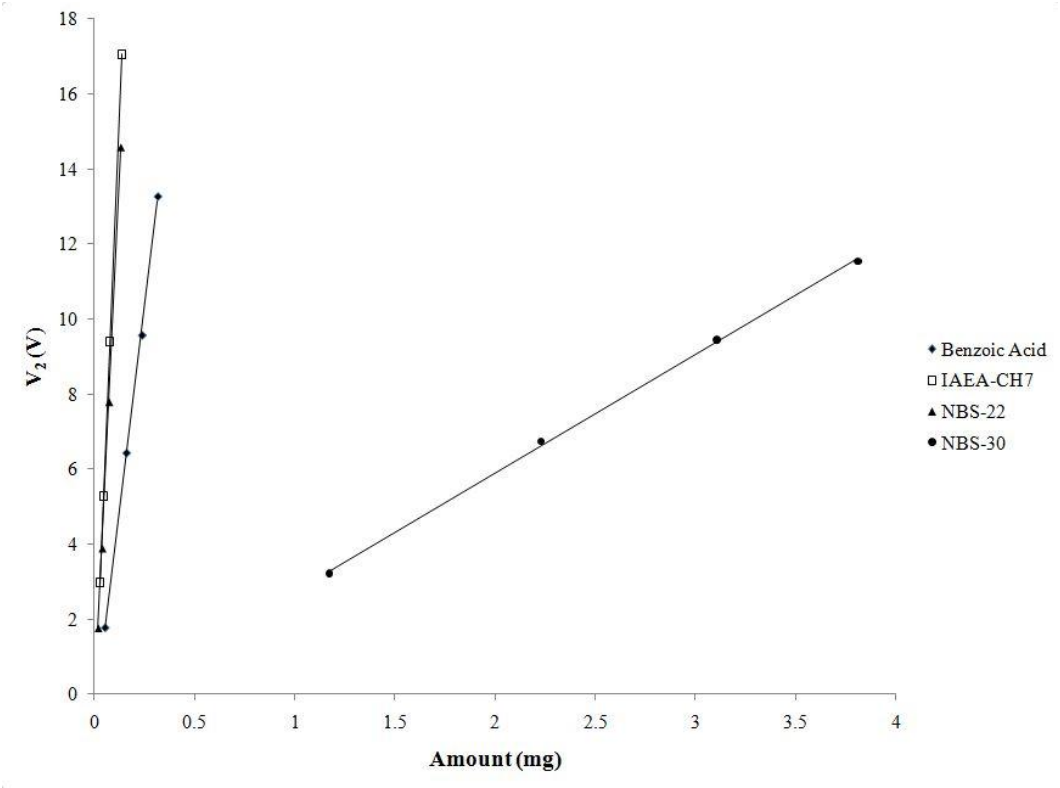

Figure 34. Comparison of sample yields for benzoic acid, IAEA CH7, NBS-22 and NBS-30. The relatively low slope of the NBS-30 data indicates that it contains less hydrogen than the other materials.

instrument. However, the effect can be negated by plotting k as a function of A_2, then using the value of k along the curve that corresponds to the value of A_2 for an unknown (Figure 35).

This variable value of the k-factor is also indicative of another issue – the helium flushing method suggested in the Thermo Finnigan TC/EA instrument manual, and employed by Sharp et al. (2001), Abruzzese et al. (2005) and Hren et al. (2009) does not entirely remove all surface water from solid samples. The effect on the observed δD is demonstrable. A plot of the ratio of $\frac{V_2}{\text{Amount}}$ as a function of Amount (mg) in Figure 36 exhibits a positive slope, indicating that as the total amount of material analyzed increases, the amount of hydrogen in the sample increases anomalously. Grain size of the analyzed material likewise seems to affect the amount of hydrogen per unit sample weight, with smaller grain sizes producing more hydrogen. This indicates that a monolayer of water adsorbed to the surface of the analyzed material and was not removed via flushing with helium. The effect on δD is illustrated in Figure 37, from data for Cretaceous chert K-400. This effect should be magnified to some extent on samples with a low amount of internal hydrogen. The results on low wt%H samples have not been determined, but it should affect the δD value by, in effect, dragging it toward to the δD value of ambient atmospheric moisture in the laboratory. The δD of the ambient moisture in the laboratory atmosphere is conservatively estimated at -100‰ VSMOW in this thesis, based upon the asymptotic approach to that value exhibited in Figure 37. Without further

investigation, however, any correction for this surface water effect would be premature.

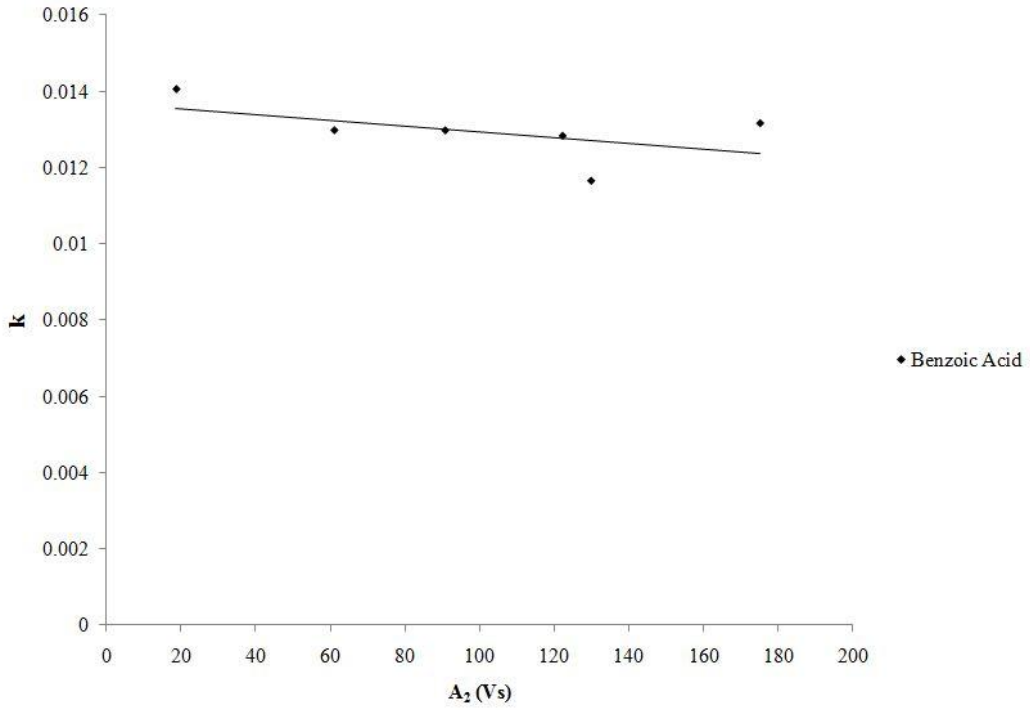

Figure 35. The ‘k-factor’ as a function of sample size in benzoic acid.

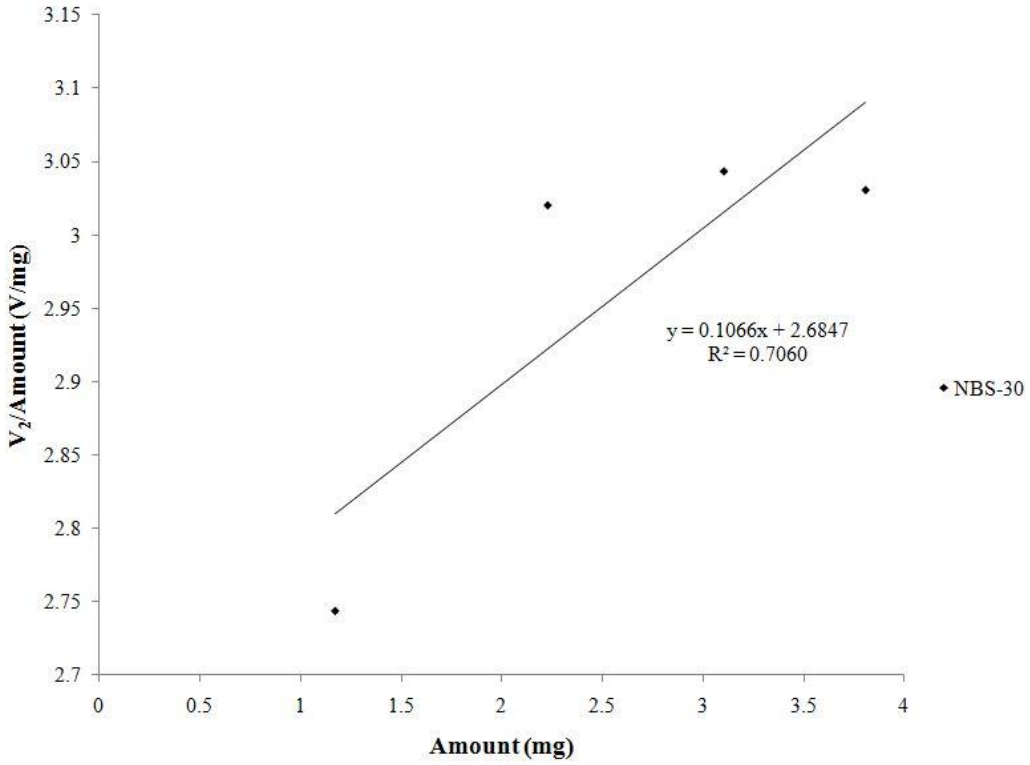

Figure 36. The rate of signal per unit sample size is plotted as a function of sample size. The positive slope indicates an anomalous increase in hydrogen content per unit sample size.

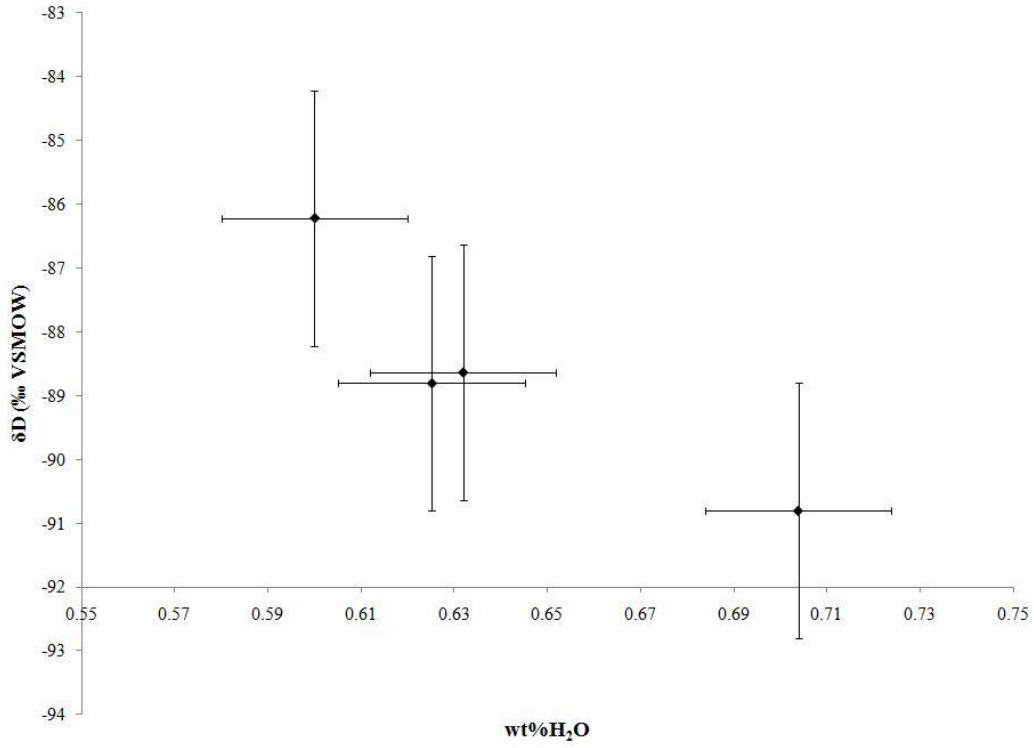

Figure 37. δD as a function of wt%H_2O for 4 different ranges of grain size. From lowest to highest wt%H_2O, the grain size ranges are 80-100, 100-200, 200-325 and >325 US Standard Mesh, respectively.

3. Application to Geologic Problems

3.1. Introduction.

The initial purpose of this thesis was to determine the maximum average surface temperature of the Earth throughout geological time following the estimation method proposed by Knauth and Epstein (1976). Knauth and Epstein (1976) began an investigation in the fields of stable isotope geochemistry and paleoclimatology by examining both the value of $\delta^{18}O$ in structurally bound oxygen in authigenic hydrous silica and the value of δD in non-stoichiometric hydroxyl groups and water contained in authigenic hydrous silica. Knauth and Epstein (1976) examined chert, which is an aggregate of hydrous, microcrystalline, granular α-quartz (the low temperature, low pressure polymorph of SiO_2), and minor amounts of chalcedony (fibrous α-quartz). The α-quartz crystals occur in the form of stacked plates approximately 600 Å thick (Micheelsen, 1966). The faces of each crystal are predominantly Si—OH groups, with a monolayer of water between adjacent plates. According to Micheelsen (1966), the hydroxyl groups do not readily exchange with D_2O above 101°C, suggesting that it is possible that in geologic settings, and following crystallization, little equilibration with surrounding groundwater occurs. After crystallization, chert is largely impermeable.

There are two primary varieties of chert that Knauth and Epstein (1976) examined in their study: nodular and bedded. Nodular chert forms at the freshwater—marine groundwater interface prior to the compaction and late diagenesis of its host rock, which is typically limestone or dolostone (Knauth, 1979). In brief, the silica that comprises the chert precipitates and replaces its host rock in ovoid or irregularly shaped masses. Bedded varieties of chert most likely represent hydrous silica tests or inorganically precipitated silica that has settled out of the water column and on to the abyssal plain of an ocean.

The $\delta^{18}O$ value of the structurally bound oxygen in chert is dependent upon the isotopic composition of the water in which the chert precipitates, as well as upon the temperature of the system during precipitation. The δD value of water and hydroxyl extracted from chert is likewise dependent upon the isotopic composition of the surrounding water as well as the temperature of the system during crystallization. If the isotopic composition of both the hydrogen and oxygen components is known, the temperature of formation, and therefore the maximum average climatic temperature, can be estimated with some degree of certainty. To this end, Knauth and Epstein followed the methods described by Epstein and Taylor (1962), as well as Friedman (1953) and Godfrey (1962) to measure both the oxygen isotope composition as well as the hydrogen isotope composition of water in chert.

Craig (1961b), extending the work begun by Epstein and Mayeda (1953) and Friedman (1953), defined the following relationship between the hydrogen

and oxygen isotope ratios of meteoric water that had not undergone extreme evaporation: $\delta D = 8\delta^{18}O + 10$. Craig (1961b) called this curve the Global Meteoric Water Line (GMWL). All of the meteoric water on Earth, with the exception of water that has undergone radical evapoconcentration, falls on the GMWL. The slope of the curve is due to Rayleigh fractionation during the evaporation and condensation of water. Knauth and Epstein (1976) discovered that plotting the value of δD measured in water from nodular chert of a given temporal range as a function of the value $\delta^{18}O$ from the bound oxygen in the same chert resulted in an elongated domain of values possessing a slope of approximately 8. Chert that had presumably precipitated in marine water with an isotopic composition approaching that of VSMOW, clustered about Line A (Figure 38). Knauth and Epstein (1976) interpreted the slope of their chert data domains as evidence that the chert had precipitated in a mixture of marine and meteoric water. The intercepts of the chert domains were negatively offset relative to the GMWL. This offset was interpreted by Knauth and Epstein (1976) as being due to mass-dependent isotopic fractionation between chert and water. The extent of the offset was attributed primarily to temperature, with a larger offset representing a relatively low temperature of precipitation. The temperature of chert formation was based upon the oxygen isotope fractionation factor between chert and water, α, where $\alpha_{chert-water} = \frac{R_{chert}}{R_{water}}$. $\alpha_{chert-water}$ was

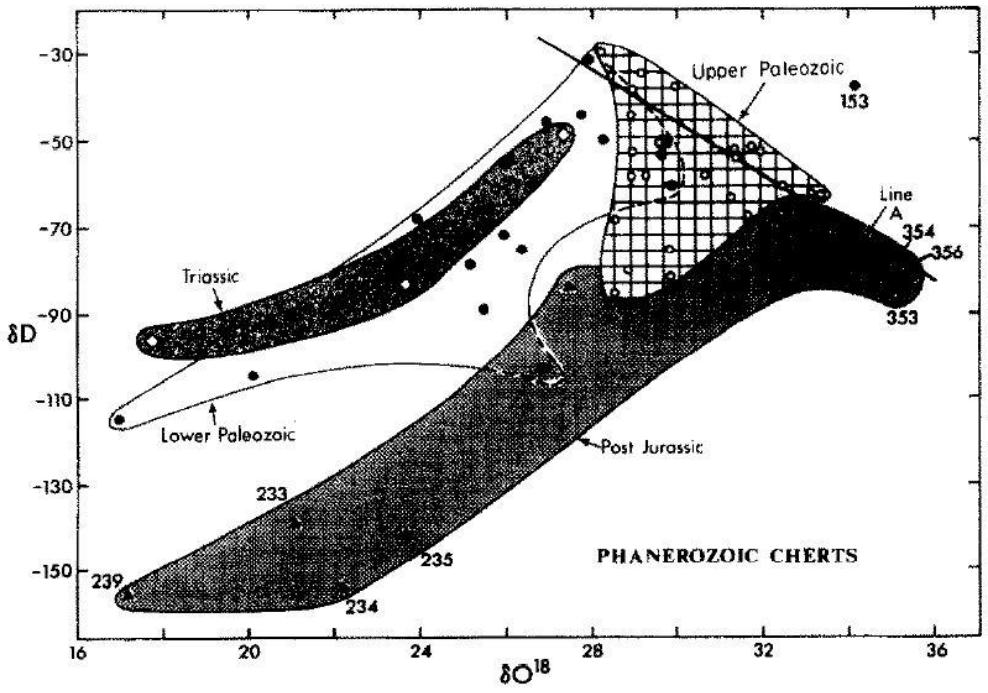

Figure 11. δD from non-stoichiometric water in chert as a function of $\delta^{18}O$ in structurally bound oxygen in chert (from Knauth and Epstein, 1976).

estimated by assuming that chert dredged from the Horizon Guyot, that had formed geologically recently, had experienced shallow burial and that its oxygen isotope ratio of $\delta^{18}O = +39‰$ (SMOW) represented an average oceanic low temperature limit near 0°C (Knauth and Epstein, 1976). From this assumption, Knauth and Epstein (1976) were able to calculate an approximate temperature of chert formation using the equation $1000\ln\alpha_{chert-water} = 3.09 \times 10^6 T^{-2} - 3.29$, where T is the temperature in °K. The resulting temperature curves are shown in Figure 39.

Knauth and Epstein (1976) concluded that chert that had formed prior to 545 Ma had equilibrated with mixed marine water and freshwater at temperatures exceeding 43°C; possibly as high as 65-70°C during the Precambrian. This temperature of formation should reflect maximum average surface temperatures, as the temperature at the depth of burial during chert formation roughly matches that of the Earth's surface. This claim had vast implications that certainly caused some controversy. However, the validity of the data was not seriously questioned. Unfortunately, more wide-ranging investigations of the δD values of cherts older than 545 Ma were not rigorously attempted. Cherts from this period contained relatively low amounts of water, and as such, very large sample sizes (on the order of several grams) were required to generate adequate amounts of hydrogen.

Hren et al. (2009), contrary to the findings of Knauth and Epstein (1976), proposed maximum average surface temperatures no greater than 40°C.

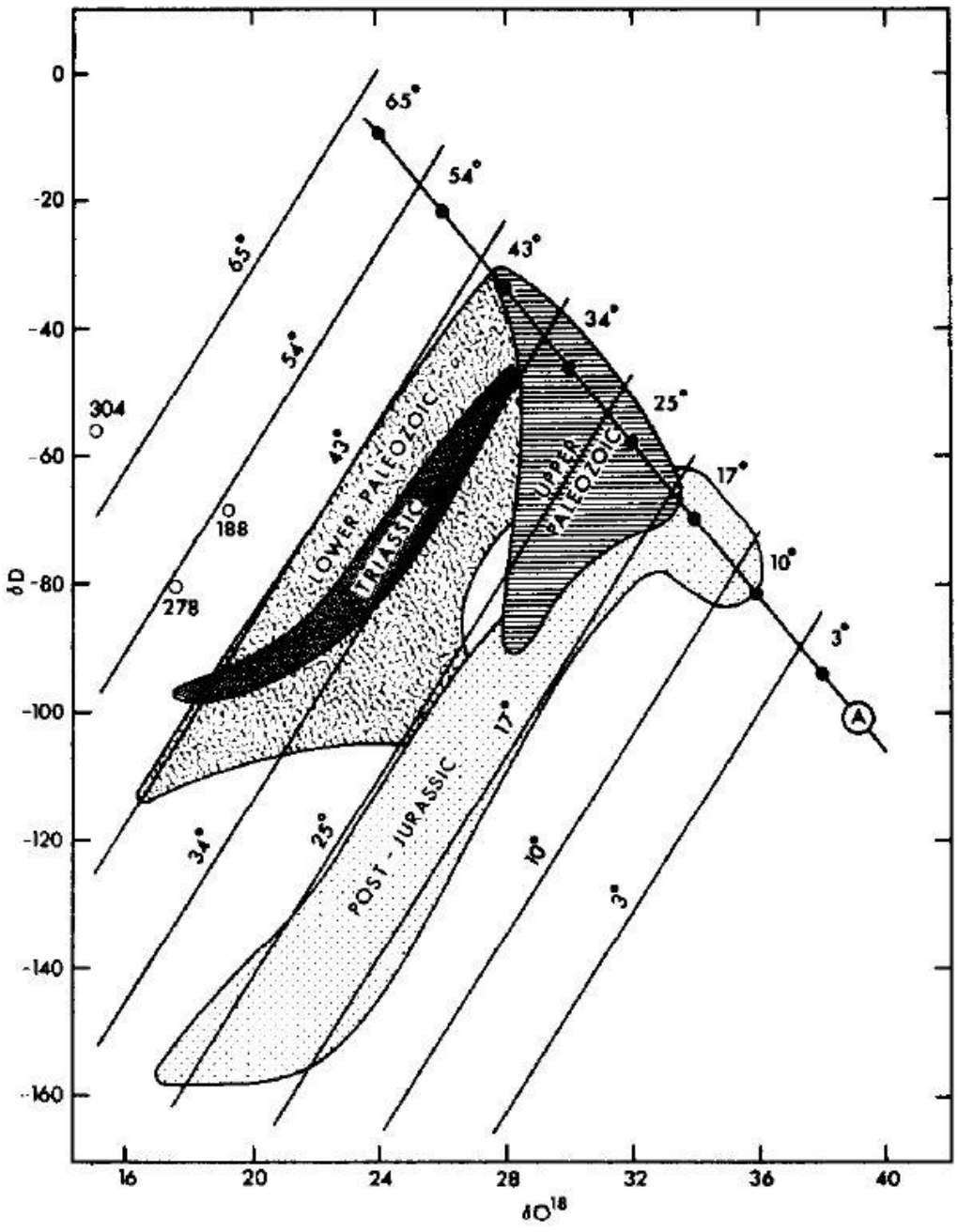

Figure 39. Figure 38 overlain by estimated temperature curves (from Knauth and Epstein, 1976).

Following both the method of analysis and data reduction proposed by Abruzzese et al. (2005) and Epstein and Taylor (1962), Hren et al. (2009) determined both the δD and $\delta^{18}O$ of water in chert from the Precambrian Buck Reef Formation in South Africa. Hren et al. (2009) measured values of δD as low as -140‰ (VSMOW), and $\delta^{18}O$ ranging from 13.3 to 20.0‰ (VSMOW). The values of δD are lower than almost any other previous measured value in water from chert (Figure 40), and are far lower than any value ever measured in chert from the Precambrian. From these values, Hren et al. (2009) proposed a new isothermal exchange path during rock-water interaction, as well as a temperate climate during the Precambrian (Figure 41). However, based upon questionable data reduction techniques used in Abruzzese et al. (2005) and data presented in this thesis, the work of Hren et al. (2009) deserves further scrutiny.

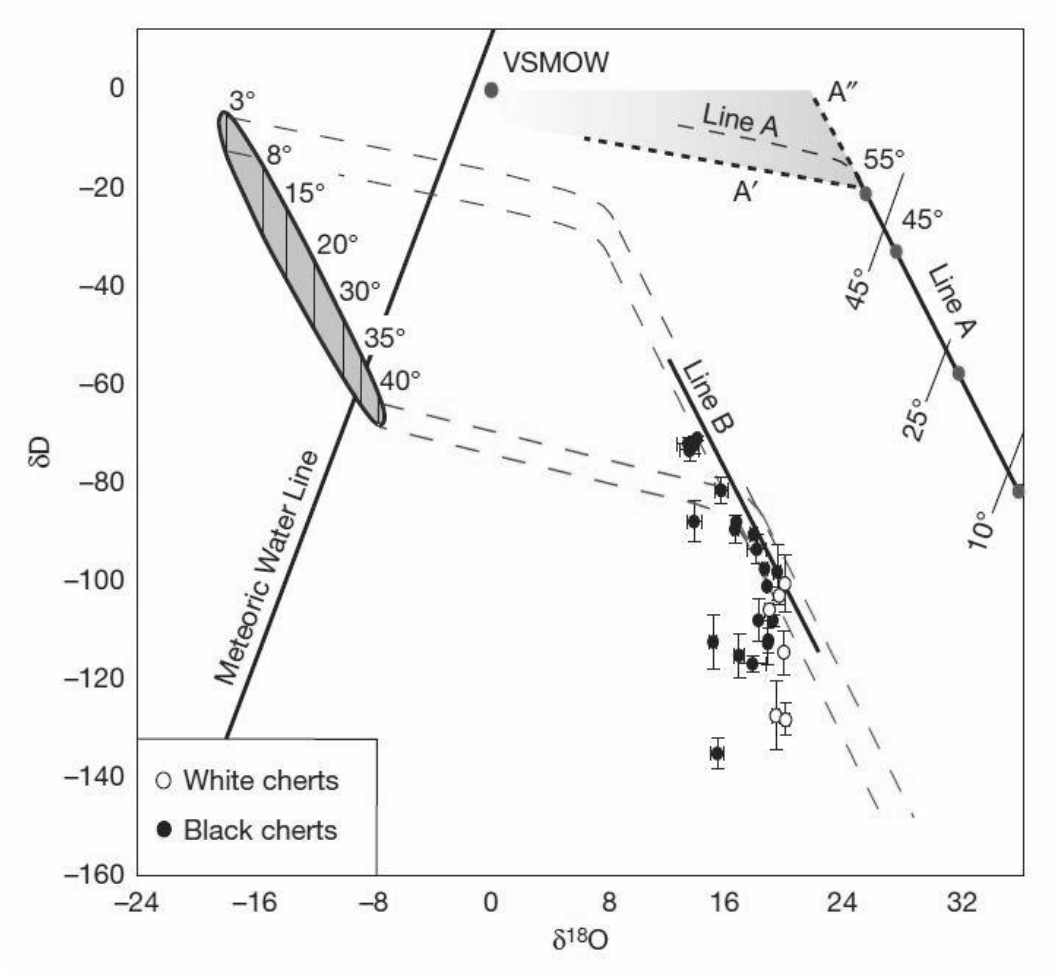

Figure 40. New proposed bounding line, Line B, based upon an isotopic composition of the Precambrian ocean that is considerably different from the current value (from Hren et al., 2009).

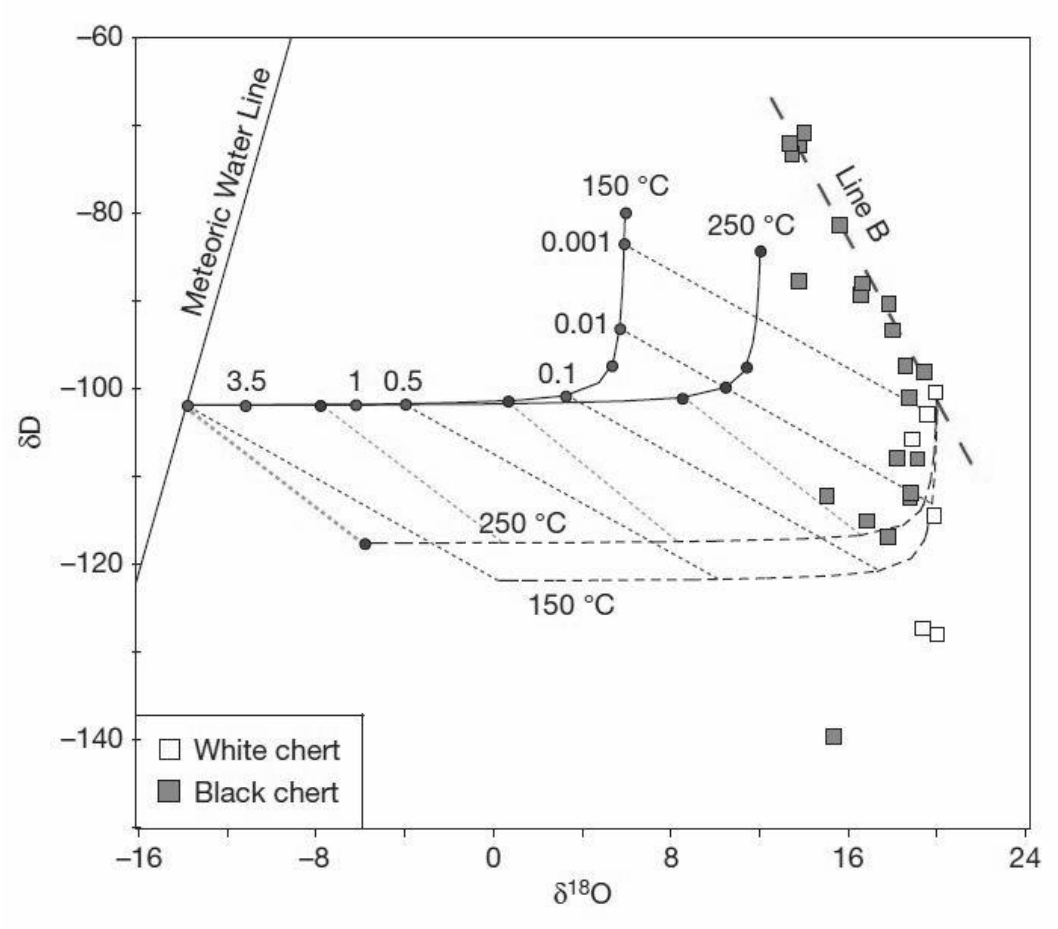

Figure 41. Isotopic exchange pathway proposed by Hren et al. (2009) to account for low values of δD.

3.2. Cretaceous Chert

Nodular chert from the Cretaceous Edwards Group, Texas, were prepared for isotopic analysis by first crushing large samples with a rock hammer. Small chips for further processing were chosen in order to represent the interior of the chert nodule. Chert fragments were selected based upon visual homogeneity, lack of obvious surface alteration, lack of veins of secondary silica, and lack of other inclusions. Samples were then crushed with a steel mortar and pestle and separated according to grain size. Powders falling into the 100-200 US Standard Mesh grain size range were kept for further processing. Steel fragments were removed magnetically, and the powders were soaked in dilute HCl for approximately 10 minutes to remove any remaining carbonate. The powders were then rinsed three times with deionized water and left to soak overnight in household bleach in order to remove organics as in the method of Abruzzese et al. (2005). After soaking in bleach, the chert powders were once again rinsed thoroughly in deionized water and then dried for four hours in a laboratory oven at 80°C. Prior to storage, powders were inspected in temporary grain mount with a petrographic microscope to ensure than no carbonate or clay minerals had inadvertently been included. Following inspection, powders were stored in clean vials for further use.

δD of Cretaceous cherts was determined using the method proposed by this thesis. $\delta^{18}O$ was determined using the method of Clayton and Mayeda (1963).

δD values for Cretaceous cherts of the Edwards Group, Texas, are given in Table 2. Hydrogen and oxygen isotope data for chert from this thesis, Land (1977), and Knauth and Epstein (1976) are shown in Figure 42. The approximate position of Line A, the locus for chert formed in equilibrium with VSMOW at a range of temperatures, is shown as in Knauth and Epstein (1976). Data from Land (1977) consists of hydrogen and oxygen isotope measurements for chert from the Edwards Group. As can be seen, the values determined in this thesis fall well within the range given by Land (1977). The hydrogen and oxygen isotope measurements from Knauth and Epstein (1976) consist of post-Jurassic chert data from the JOIDES DSDP; Dover Flint, England; Fredericksburg Limestone, Texas; Aguja Formation, Texas; and the Humboldt Formation, Nevada. The data from this thesis fall within this larger range of data for post-Jurassic chert given by Knauth and Epstein (1976). The few values from Land (1977) that fall above Line A are consistent with chert formation in a highly evapoconcentrated, isotopically enriched brine.

These values, and their agreement with previously published data given by Knauth and Epstein (1976) and Land (1977), indicate that the method of analysis proposed by this thesis is accurate. The chert most likely precipitated in a mixture of meteoric and marine water. The range of data provided by this thesis, as well

as Land (1977), likely represents an approximate limit for chert during the Cretaceous, reflecting maximum average surface temperatures as high as 25°C. The interpretation of this data is congruent with that proposed by Knauth and Epstein (1976) as well as Land (1977).

Table 2. δD and $\delta^{18}O$ in Cretaceous Chert (VSMOW).

Sample ID	$\delta^{18}O$ (‰)	δD (‰)	No.	σ (δD)	wt% H_2O
K-400	33.0	-86	6	0.63	0.73
K-422	33.7	-78	6	1.13	1.01
K-407	34.0	-79	6	1.01	0.83
K-432	30.5	-91	6	1.55	0.44
K-461	31.8	-76	6	6.53	0.76
K-413	33.1	-79	6	1.76	1.02
K-421	33.0	-78	6	0.72	1.04
K-400	32.5	-86	6	1.74	0.76
K-433	29.1	-75	6	0.84	0.70
K-457	30.4	-79	6	0.84	0.72

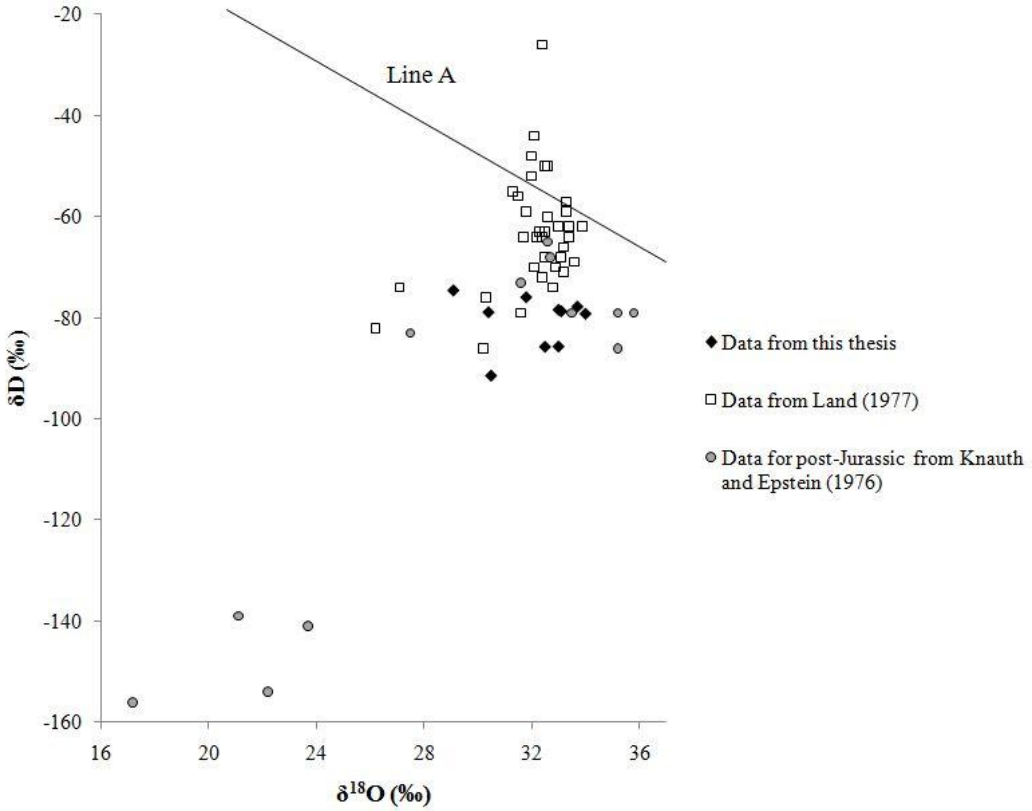

Figure 42. δD as a function of $\delta^{18}O$ in Cretaceous chert from the Edwards Group as measured in this thesis and Land (1977), as well as other post-Jurassic chert from Knauth and Epstein (1976).

3.3. Archean Basalt.

Archean basalts were powdered with an agate mortar and pestle, rinsed thoroughly with deionized water and dried in a laboratory oven at 80°C. Samples were stored in clean vials for further use. Basalts were analyzed for δD and wt%H_2O using the analytical method proposed in this thesis. $\delta^{18}O$ and other geochemical data were provided by Karlis Muehlenbachs (personal communication).

The basalts were sampled from the uppermost portion of the Hooggenoeg Complex, South Africa. A recent interpretation of the geological background as well as the geographic location are given in de Wit et al. (2011) and Furnes et al. (2011). De Wit et al. (2011) propose an extensive new nomenclature that supersedes previous work. Regardless, the basalts analyzed in this study are taken from section HV15 of the Hooggenoeg Complex (de Wit et al, 2011; Furnes et al., 2011). Nearly all of the rocks within HV15 are variole-bearing pillow basalts, representing ocean-floor basalt, while the section is capped by the Buck Reef Chert. Detailed petrology of the basalt portions of the formation are given in Furnes et al. (2011), whereas detailed petrology of the chert is given in Lowe (1999). Figure 43 (from Furnes et al., 2011) gives a stratigraphic sequence of section HV15 of the Hooggenoeg Complex. Approximate stratigraphic location of the samples is given next to the illustration. Lighter portions of the figure represent variole-bearing pillow basalts and the darker portions represent more

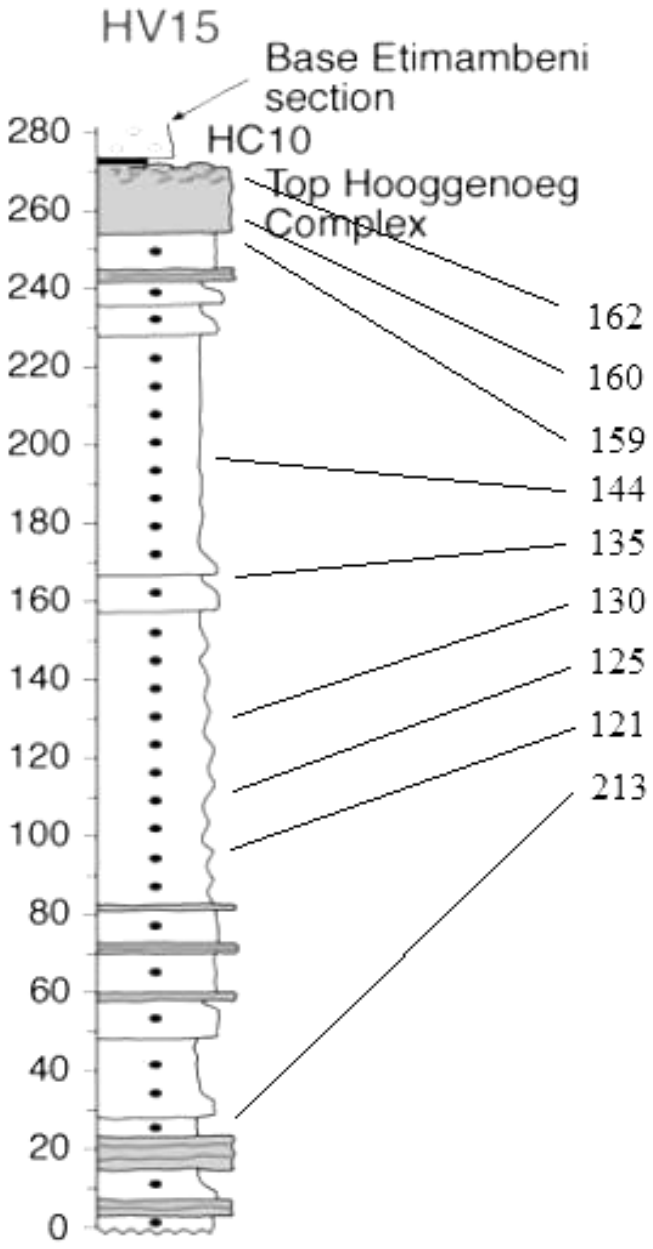

Figure 43. Stratigraphic column indicating the location of analyzed basalts in HV15 of the Hooggenoeg Complex, South Africa (adapted from Furnes et al., 2011).

massive basalt flows. Based upon oxygen isotope data, all of the basalt has been hydrothermally altered to chlorite and silica at temperatures between 100 and 400°C (Karlis Muehlenbachs, personal communication). Figure 44 illustrates the δD values of the basalt samples as a function of $\delta^{18}O$. There appears to be little to no correlation between the oxygen and hydrogen isotope ratios of the basalt samples. δD and wt%H_2O are compiled in Table 3. Again, there appears to be little to no correlation between the water content and hydrogen isotope ratios of the basalt samples (Figure 45).

It is possible that these D/H values represent the hydrogen isotope composition of the mantle, or that they reflect the isotope composition of a metamorphic fluid. However, based upon the interpretations of similar systems by Wenner and Taylor (1974), and based upon the geological interpretations provided by de Wit et al. (2011) and Furnes et al. (2011), it is likely that these δD values represent early alteration values and presumably record the δD of the alteration fluid in a large hydrothermal system. Based upon data for fractionation factors of similar minerals i1n Suzuoki and Epstein (1976), and the fractionation factor data for chlorite given in both Marumo et al. (1980) and Saccocia et al. (2009), the range of δD for the basalt samples are expected if the value of the alteration fluid is approximately 0‰ (VSMOW) and the alteration occurred at temperatures between 100 to 400 °C. Assuming these measurements are accurate, the δD of the Archean ocean during the period of diagenesis may have approached the contemporary value. If so, this would obviate the isotopic

exchange pathway and negate the estimated isotopic composition of the Archean ocean proposed by Hren et al. (2009).

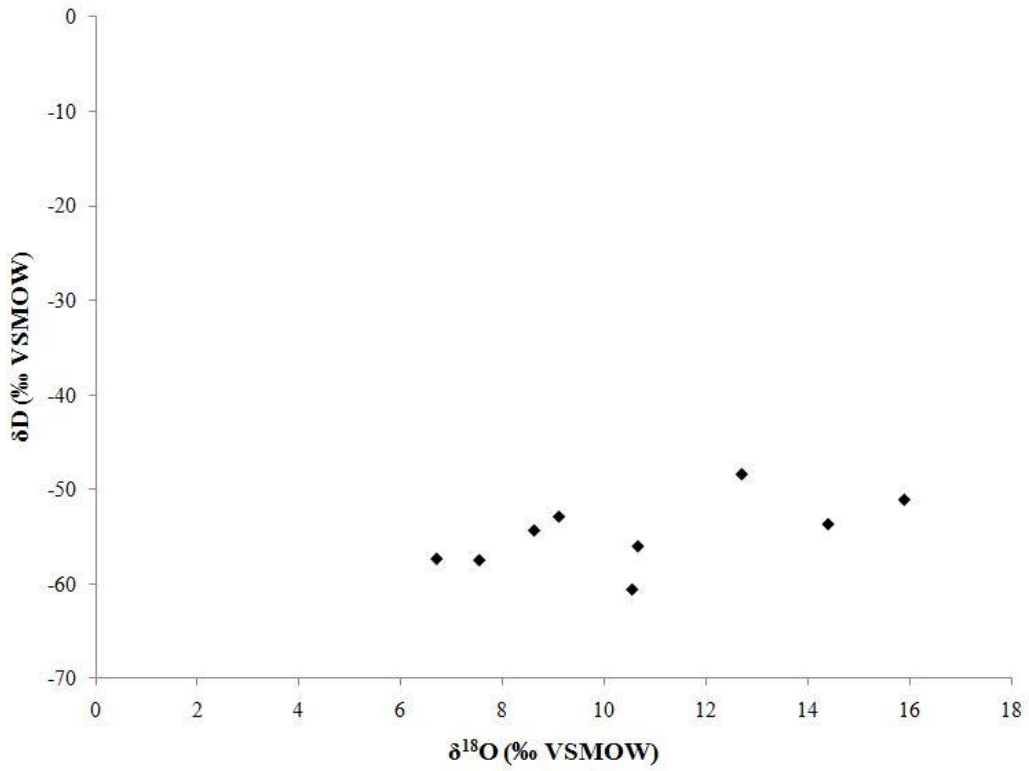

Figure 44. δD as a function of $\delta^{18}O$ in analyzed basalts from the Hooggenoeg Complex, South Africa.

Table 3. Compiled hydrogen isotope data for analyzed basalts from HV15 in the Hooggenoeg Complex, South Africa.

Sample ID	wt%H_2O	δD (‰ VSMOW)	No.	σ
121	6.906	-57	5	0.794
125	1.011	-56	5	1.882
130	2.259	-61	4	1.073
135	6.559	-58	6	0.842
144	8.768	-53	4	0.486
159	3.292	-48	6	1.790
160	4.889	-54	5	0.611
162	1.817	-51	4	0.545
213	1.863	-54	4	0.900

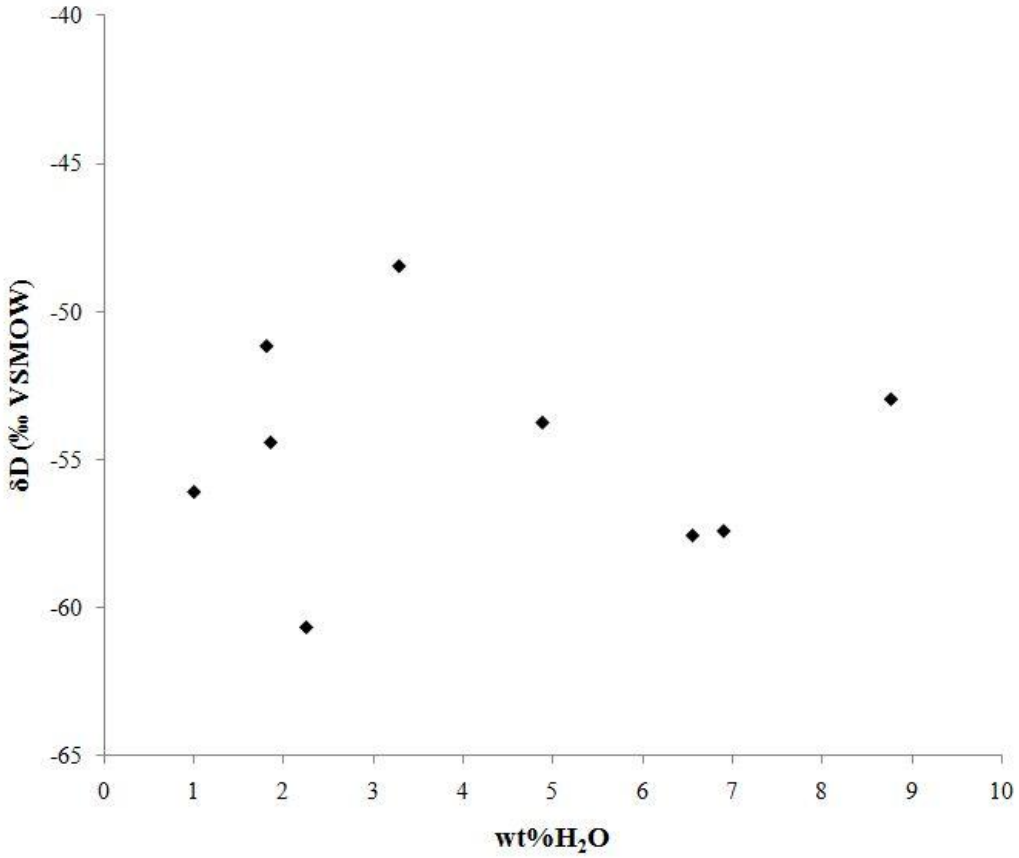

Figure 45. δD as a function of wt%H_2O in analyzed basalts from HV15 in the Hooggenoeg Complex, South Africa.

3.4. Archean Chert.

Archean chert samples were prepared for analysis following the method described for the Cretaceous chert samples. Archean chert samples were prepared for isotopic analysis by first crushing large samples with a rock hammer. Small chips for further processing were chosen in order to represent the interior of the chert sample. Chert fragments were selected based upon visual homogeneity, lack of obvious surface alteration, lack of veins of secondary silica, and lack of other inclusions. Samples were then crushed with a steel mortar and pestle and separated according to grain size. Powders falling into the 100-200 US Standard Mesh grain size range were kept for further processing. Steel fragments from the mortar and pestle were removed magnetically, and the powders were soaked in dilute HCl for approximately 10 minutes to remove any remaining carbonate. The powders were then rinsed three times with deionized water and left to soak overnight in household bleach in order to remove organics, as in the method of Abruzzese et al. (2005). The chert powders were once again rinsed thoroughly in deionized water and then dried for four hours in a laboratory oven at 80°C. Prior to storage, powders were inspected in temporary grain mount with a petrographic microscope to ensure than no carbonate or clay minerals had been inadvertently included. Powders were then stored in clean vials for further use.

The δD values of Archean chert samples were determined using the method proposed by this thesis. $\delta^{18}O$ values were determined using the method of Clayton and Mayeda (1963).

Two Archean cherts were sampled. Both were from the Archean Kromberg Formation, South Africa. One of the cherts, the Buck Reef Chert, serves as the upper limit to the sampled basalts in the previous chapter, and is the lower bound of the Kromberg Formation. The other, the Footbridge chert serves as the cap rock for Kromberg Formation. The δD value of the Buck Reef Chert was -53‰ (VSMOW), with a standard deviation of 7.57 after 6 analyses. The Buck Reef Chert contained approximately 0.23 wt%H_2O. The δD value of the Footbridge Chert was -58‰ (VSMOW), with a standard deviation of 11.85 after 5 analyses. The Footbridge Chert sample contained approximately 0.121 wt%H_2O.

Despite the poor reproducibility of the chert data, even at a minimum depleted value of -70‰ (VSMOW) it is equal to the most enriched value put forth in Hren et al. (2009). The Buck Reef chert sample possessed a $\delta^{18}O$ value of 19.1‰ (VSMOW). The Footbridge chert sample possessed a $\delta^{18}O$ value of 20.0‰ (VSMOW) (Karlis Muehlenbachs, personal communication, unpublished data). As illustrated in Figure 46, both of these values plot above the Line B proposed by Hren et al. (2009) by approximately 50‰, and are consistent with maximum average surface temperatures ca. 3.4 Ga above 55°C and possibly as high as 65°C (Knauth and Epstein, 1976) (Figure 39).

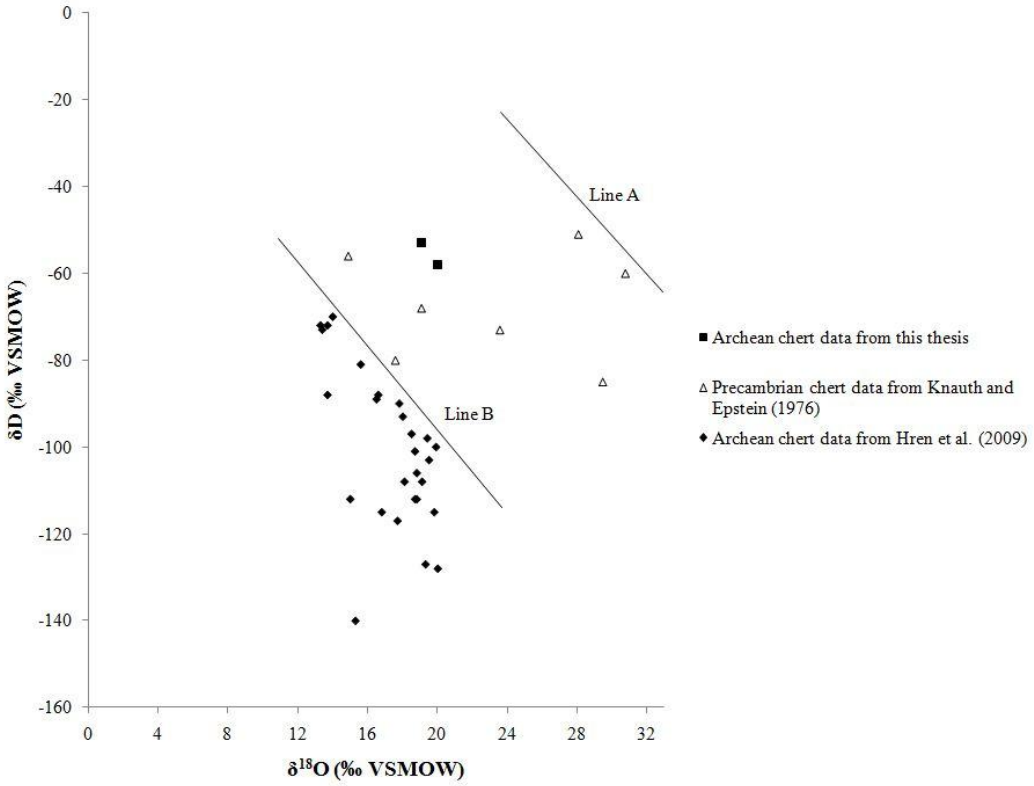

Figure 46. Chert data from this thesis, Knauth and Epstein (1976), and Hren et al. (2009). The approximate positions of both Line A (Knauth and Epstein, 1976) and Line B (Hren et al., 2009) are shown.

The water content of the Archean chert samples, as measured in this thesis, is much lower than many of those reported by Hren et al. (2009). Hren et al. (2009) reported that they kept all chert powder passing 175 US Standard Mesh for analysis. It is possible that using a shatterbox (Abruzzese et al., 2005; Hren et al., 2009) and keeping all powder that passed 175 mesh created a high proportion of chert grains with a significant surface area to volume ratio. As indicated earlier in this thesis, as grain size increases, δD decreases and water content increases. Presumably, this grain size effect would be even more pronounced as internal water content decreases. Although Hren et al. (2009) reported no correlation between water content and δD, they did not compare water content and δD when sample composition was kept constant and grain size was varied. Furthermore, although Hren et al. (2009 Supplementary Material) reported no measurable effect in surface exchange experiments, they dried all of their samples in a vacuum oven prior to inserting the samples into the helium-flushed autosampler. Drying in the vacuum oven would have removed the D-enriched water used in the surface exchange experiments, while exposure to the laboratory atmosphere during transfer to the autosampler would have caused surface hydration by isotopically depleted ambient moisture. Finally, at the sample sizes reported by Hren et al. (2009), it is possible that the data are simply unreliable in that they fall within the sample size range where data is often irreproducible, according to the evaluation of the method used Abruzzese et al. (2005) given in this thesis.

Based upon the δD values and low water content reported in this thesis, the demonstrable effect that grain size has upon δD, and the evaluation of the analytical method used by both Abruzzese et al. (2005) and Hren et al. (2009), it is possible that the chert data produced by Hren et al. (2009) largely reflect the δD value of adsorbed surface water. From their data, Hren et al. (2009) propose an alternate isotopic exchange pathway based upon a unique isotopic composition of the ocean during the Archean. In addition, Hren et al. (2009) propose a new bounding line, Line B, for chert data. Finally, Hren et al. (2009), based upon a variable isotopic composition of the ocean and Line B, propose a temperate climate during the Archean. However, Hren et al. (2009) fail to account for previously published data that negate their hypotheses and fail to account for the issues raised by this thesis. If the data and interpretations provided in this thesis are accurate, it is clear that the data and hypotheses proposed by Hren et al. (2009) should be reevaluated.

4. Conclusions

Although the use of pyrolysis facilitated GC-IRMS to measure D/H in non-stoichiometric water from naturally occurring solid samples was reported as early as 2001 by Sharp et al., it is clear that further evaluation of both published analytical methods and data is warranted. Based upon the data collected and presented in this thesis, several conclusions can be reached:

(1) The calculation methods used by the computer program, Isodat, to calculate δD-values as well as the H_3^+-factor is flawed. The analytical method proposed by Sharp et al. (2001) is prone to selection bias and, even if effective at times, is ad hoc. The analytical method used by Abruzzese et al. (2005) is likewise prone to selection bias. The method proposed by this thesis, in which the instantaneous isotope ratio at the maximum amplitude of V_2 is used to calculate the H_3^+-factor is well supported by the data in this thesis, is based upon first principles of hydrogen isotope mass spectrometry, and produces data that is both precise and accurate.

(2) An examination of the data used to calculate wt%H_2O indicates that despite long durations of high purity helium flushing while in the Costech Zero Blank Autosampler, a small amount of adsorbed surface water remains on samples. Drying in a vacuum oven prior to analysis likely does not help to resolve this, as the samples are exposed to atmosphere during the sample loading process. Grain size also appears to be an issue, as smaller grain sizes have a higher surface area to volume ratio, increasing the proportion of adsorbed surface water analyzed per

given unit of sample size. The effect has been demonstrated and appears to cause a decrease in δD and an increase in water content as grains size decreases.

(3) The Cretaceous cherts analyzed in this thesis provide confirmation that the analytical method proposed in this thesis is both accurate and precise.

(4) Data from Archean basalts is consistent with δD of the Archean ocean similar to the contemporary value.

(5) Despite being a small sample suite, data from Archean cherts provided by this thesis directly contradict the values and hypotheses proposed by Hren et al. (2009), warranting further investigation of Precambrian cherts and further evaluation of data produced by Hren et al. (2009). Moreover, it is in the best interests of the field of stable isotope geochemistry for any future chert studies to begin with cherts that contain a high amount of internal water (post-Jurassic), and then work back to cherts that contain lesser amounts of internal water (Precambrian). Simply beginning with the most difficult samples using a largely untested technique has led to problematic conclusions.

The analytical method proposed in this thesis elucidates heretofore undetected or unsolved problems in the analytical methods used in Sharp et al. (2001), Abruzzese et al. (2005) and Hren et al. (2009). The results of this thesis demand a reevaluation of previously published data in which D/H is measured using pyrolysis facilitated GC-IRMS.

REFERENCES

Abruzzese, M.J., Waldbauer, J.R., Chamberlain, C.P., 2005. Oxygen and hydrogen isotope ratios in freshwater chert as indicators of ancient climate and hydrologic regime. Geochimica et Cosmochimica Acta, 69, 1377-1390.

Begley, I.S., Scrimgeour, C.M., 1997. High-precision δ^2H and $\delta^{18}O$ measurement for water and volatile organic compounds by continuous-flow pyrolysis isotope ratio mass spectrometry. Analytical Chemistry, 69, 1530-1535.

Bigeleisen, J., Perlman, M.L., Prosser, H.C., 1952. Conversion of hydrogenic materials to hydrogen for isotopic analysis. Analytical Chemistry, 24, 1356-1357.

Burgoyne, T.W., Hayes, J.M., 1998. Quantitative production of H_2 by pyrolysis of gas chromatographic effluents. Analytical Chemistry, 70, 5136-5141.

Clayton, R.N., Mayeda, T.K., 1963. The use of bromine pentafluoride in the extraction of oxygen from oxides and silicates for isotopic analysis. Geochimica et Cosmochimica Acta, 27, 43-52.

Craig, Harmon, 1961a. Standard for reporting concentrations of deuterium and oxygen-18 in natural waters. Science, 133, 1833-1834.

Craig, Harmon, 1961b. Isotopic variations in meteoric waters. Science, 133, 1702-1703.

Eiler, J.M., Kitchen, N., 2001. Hydrogen-isotope analysis of nanomole (picoliter) quantities of H_2O. Geochimica et Cosmochimica Acta, 65, 4467-4479.

Friedman, I., 1953. Deuterium content of natural waters and other substances. Geochimica et Cosmochimica Acta, 4, 89-103.

Godfrey, J.D., 1962. The deuterium content of hydrous minerals from the East-Central Sierra Nevada and Yosemite National Park. Geochimica et Cosmochimica Acta, 26, 1215-1245.

Greule, M., Mosandl, A., Hamilton, J.T.G., Keppler, F., 2008. A rapid and precise method for determination of D/H ratios of plant methoxyl groups. Rapid Communications in Mass Spectrometry, 22, 3983-3988.

Hren, M.T., Tice, M.M., Chamberlain, C.P., 2009. Oxygen and hydrogen isotope evidence for a temperate climate 3.42 billion years ago. Nature, 462, 205-208.

Knauth, L.P., 1979. A model for the origin of chert in limestone. Geology, 7, 274-277.

Knauth, L.P., Epstein, S., 1976. Hydrogen and oxygen isotope ratios in nodular and bedded cherts. Geochimica et Cosmochimica Acta, 40, 1095-1108.

Knauth, L.P., Epstein, S., 1982. The nature of water in hydrous silica. American Mineralogist, 67, 510-520.

Lambert, S.J., Epstein, S., 1980. Stable isotope investigations of an active geothermal system in Valles Caldera, Jemez Mountains, New Mexico. Journal of Volcanology and Geothermal Research, 8, 111-129.

Land, L.S., 1977. Hydrogen and oxygen isotopic composition of chert from the Edwards Group, lower Cretaceous, central Texas. Cretaceous Carbonates of Texas & Mexico: Applications to Subsurface Exploration, 89, 202-205.

Matthews, D.E., Hayes, J.M., 1978. Isotope-ratio-monitoring gas chromatography-mass spectrometry. Analytical Chemistry, 50, 1465-1473.

McKinney, C.R., McCrea, J.M., Epstein, S., Allen, H.A., Urey, H.C., 1950. Improvements in mass spectrometers for the measurement of small differences in isotope abundance ratios. The Review of Scientific Instruments, 21, 724-730.

Micheelsen, H. 1966. The structure of Dark Flint from Stevns, Denmark. Medd. Dansk Geol. Foren. 16, 284-397.

Nier, A.O., 1947. A mass spectrometer for isotope and gas analysis. The Review of Scientific Instruments, 18, 398-411.

Prosser, S.J., Scrimgeour, C.M., 1995. High-precision determination of $^{2}H/^{1}H$ in H_2 and H_2O by continuous-flow isotope ratio mass spectrometry. Analytical Chemistry, 67, 1992-1997.

Ricci, M.P., Merritt, D.A., Freeman, K.H., Hayes, J.M., 1994. Acquisition and processing of data for isotope-ratio-monitoring mass spectrometry. Organic Geochemistry, 21, 561-571.

Sessions, A.L., Burgoyne, T.W., Schimmelmann, A., Hayes, J.M., 1999. Fractionation of hydrogen isotopes in lipid biosynthesis. Organic Geochemistry, 30, 1193-1200.

Sessions, A.L., Burgoyne, T.W., Hayes, J.M., 2001a. Correction of H_3^+ contributions in hydrogen isotope ratio monitoring mass spectrometry. Analytical Chemistry, 73, 192-199.

Sessions, A.L., Burgoyne, T.W., Hayes, J.M., 2001b. Determination of the H_3 factor in hydrogen isotope ratio monitoring mass spectrometry. Analytical Chemistry, 73, 200-207.

Sharp, Z., 2007. Principles of Stable Isotope Geochemistry.

Sharp, Z.D., Atudorei, V., Durakiewicz, T., 2001. A rapid method for determination of hydrogen and oxygen isotope ratios from water and hydrous minerals. Chemical Geology, 178, 197-210.

Suzuoki, T., Epstein, S. Hydrogen isotope fractionation between OH-bearing minerals and water. Geochimica et Cosmochimica Acta, 40, 1229-1240.

Smyth, H.D., 1931. Products and processes of ionization by low speed electrons. Reviews of Modern Physics, 3, 347-392.

Taylor Jr., H.P., Epstein, S., 1962. Relationship between O^{18}/O^{16} ratios in coexisting minerals of igneous and metamorphic rocks. Geological Society of America Bulletin, 73, 461-480.

Tobias, H.J., Brenna, J.T., 1996a. Correction of ion source nonlinearities over a wide signal range in continuous-flow isotope ratio mass spectrometry of water-derived hydrogen. Analytical Chemistry, 68, 2281-2286.

Tobias, H.J., Brenna, J.T., 1996b. High-precision D/H measurement from organic mixtures by gas chromatography continuous-flow isotope ratio mass spectrometry using a palladium filter. Analytical Chemistry, 68, 3002-3007.

Tobias, H.J., Goodman, K.J., Blacken, C.E., Brenna, J.T., 1995. High-precision D/H measurement from hydrogen gas and water by continuous-flow isotope ratio mass spectrometry. Analytical Chemistry, 67, 2486-2492.

Urey, H.C., 1948. Oxygen isotopes in nature and in the laboratory. Science, 108, 489-496.

Van Hook, W.A., 1967. Isotope effects on vaporization from the adsorbed state. The Journal of Physical Chemistry, 71, 3270-3275.

Wenner, D.B. Taylor Jr., H.P., 1974. D/H and O^{18}/O^{16} studies of serpentinization of ultramafic rocks. Geochimica et Cosmochimica Acta, 38, 1255-1286.

Werner, R.A., Kornexl, B.E., Roβmann, A., Schmidt, H.-L. On-line determination of $\delta^{18}O$ values of organic substances. Analytica Chimica Acta, 319, 159-164.